Scilight

Medical Materials Research

https://www.sciltp.com/journals/mmr

Review

Classification, Characteristics and Biological Applications of Inorganic Nanomaterials

Lili Liu, Yanqiu Duan and Meiqi Chang *

Laboratory Center, Shanghai Municipal Hospital of Traditional Chinese Medicine, Shanghai University of Traditional Chinese Medicine, Shanghai 200071, China

* Correspondence: changmeiqi@vip.sina.com

How To Cite: Liu, L.; Duan, Y.; Chang, M. Classification, Characteristics and Biological Applications of Inorganic Nanomaterials. *Medical Materials Research* **2025**, *1*(1), 3.

Received: 14 January 2025
Revised: 18 February 2025
Accepted: 20 February 2025
Published: 4 March 2025

Abstract: The application of inorganic nanomaterials in disease has attracted increasing attention, particularly in the areas of bioimaging, antibacteria and disease treatment. Due to their unique physicochemical properties, such as good biocompatibility, adjustable surface characteristics and excellent stability, inorganic materials have become an important component in drug delivery systems and nanomedicine. Common inorganic materials serve not only to effectively deliver drugs and facilitate controlled release within the body, but also to enhance their biological effects through specific functionalization strategies. This review aims to provide a comprehensive analysis of the latest advancements in the field of inorganic nanomaterials. The categorization and properties of inorganic nanomaterials are presented to elucidate potential structure-function relationships. Additionally, the engineering of inorganic nanomaterials for biomedical applications is comprehensively summarized. Finally, the current challenges and future directions are discussed and projected to foster technological advancements in the efficient treatment of diseases.

Keywords: inorganic nanomaterials; biomedical applications; nanomedicine; disease treatment

1. Introduction

Inorganic materials have been widely used in many fields such as energy, environment, electronics, catalysis and biomedicine due to their excellent physical and chemical properties, including high stability, high adjustability and excellent biocompatibility. Inorganic nanomaterials possess adjustable size, surface properties, and shapes, enabling targeted drug delivery through modification [1]. By surface functionalization, they can bind to specific cells or tissues, increasing the drug concentration at the target site while minimizing damage to healthy tissues [2]. For example, inorganic nanomaterials like metal oxides and metal sulfides can be functionalized to carry drugs for tumor-targeted therapy, effectively enhancing the therapeutic efficacy of anticancer drugs and reducing the side effects of chemotherapy [3,4]. Inorganic nanomaterials can not only serve as drug carriers but can also directly participate in disease treatment. For instance, metal nanoparticles (such as gold and silver nanoparticles) possess excellent antimicrobial properties, making them useful for infection treatment [5,6]. Furthermore, some inorganic nanomaterials (such as gold nanoparticles and ferrite nanoparticles) exhibit significant optical or magnetic properties, which can be used in medical imaging techniques [7,8]. The surface of inorganic nanomaterials can be chemically modified or physically encapsulated to regulate the rate of drug release. This precise release mechanism enables drugs to be released at specific times and locations, improving the targeting and effectiveness of treatments [9]. For example, pH-responsive, temperature-responsive, or enzyme-responsive nanomaterials can be used to specifically respond to the tumor microenvironment (TME), precisely control drug release and reduce toxicity to normal cells [10]. Although inorganic nanomaterials have shown many advantages in the biomedical field, their

long residence time in the body may increase the risk of harmful toxicity. This risk mainly stems from the accumulation of materials, slow metabolism or long-term interaction with biological systems, which may lead to inflammation, tissue damage or other adverse reactions [11]. Therefore, when applying inorganic nanomaterials, great attention must be paid to their degradation characteristics and clearance mechanisms.

These materials can achieve bioimaging, antibacterial and disease treatment through precise design and functionalization at the nanoscale, thereby greatly improving therapeutic effects and significantly reducing side effects. Inorganic nanomaterials perform well in biological imaging and diagnosis. For example, quantum dots (QDs) are used for high-resolution fluorescence imaging (FLI) due to their excellent optical properties [12]; superparamagnetic iron oxide nanoparticles are used as magnetic resonance imaging (MRI) contrast agents to improve the sensitivity and accuracy of disease diagnosis [13]; gold nanorods and upconversion nanoparticles have shown unique advantages in photoacoustic imaging (PAI) and multimodal imaging [14,15]. These materials provide strong technical support for early detection and accurate diagnosis of diseases. In antibacterial applications, inorganic nanomaterials such as silver peroxide, zinc oxide nanoparticles, and copper nanoparticles exhibit strong antibacterial activity. They effectively inhibit bacterial growth and even fight multidrug-resistant bacteria by destroying bacterial cell membranes, interfering with bacterial metabolism, or producing reactive oxygen. These materials are widely used in wound dressings, medical device coatings and antibacterial coatings, providing new solutions for the prevention and treatment of infections [16–18]. In the field of cancer treatment, inorganic nanomaterials have shown great potential. For example, gold nanoparticles and iron oxide nanoparticles can be used in photothermal therapy (PTT), which selectively kill cancer cells by absorbing near-infrared (NIR) light to generate local high temperatures [7,13]; titanium dioxide nanoparticles are used as photosensitizers in photodynamic therapy (PDT), which produce reactive oxygen species (ROS) under light and induce apoptosis of cancer cells [19]; mesoporous silica nanoparticles are ideal carriers of chemotherapy drugs due to their high drug loading and controlled release properties [20]. In addition, inorganic nanomaterials can also achieve active targeting through surface modification, accurately deliver drugs to the tumor site, improve the treatment effect and reduce damage to normal tissues [21].

This review systematically introduced the classification and unique properties of inorganic nanomaterials, and comprehensively summarizes their wide range of uses in biomedical applications, including bioimaging, antibacterial, disease treatment, etc. Through precise design and functionalization at the nanoscale, inorganic nanomaterials have demonstrated high stability, adjustability and versatility, providing innovative solutions for modern medicine (Figure 1).

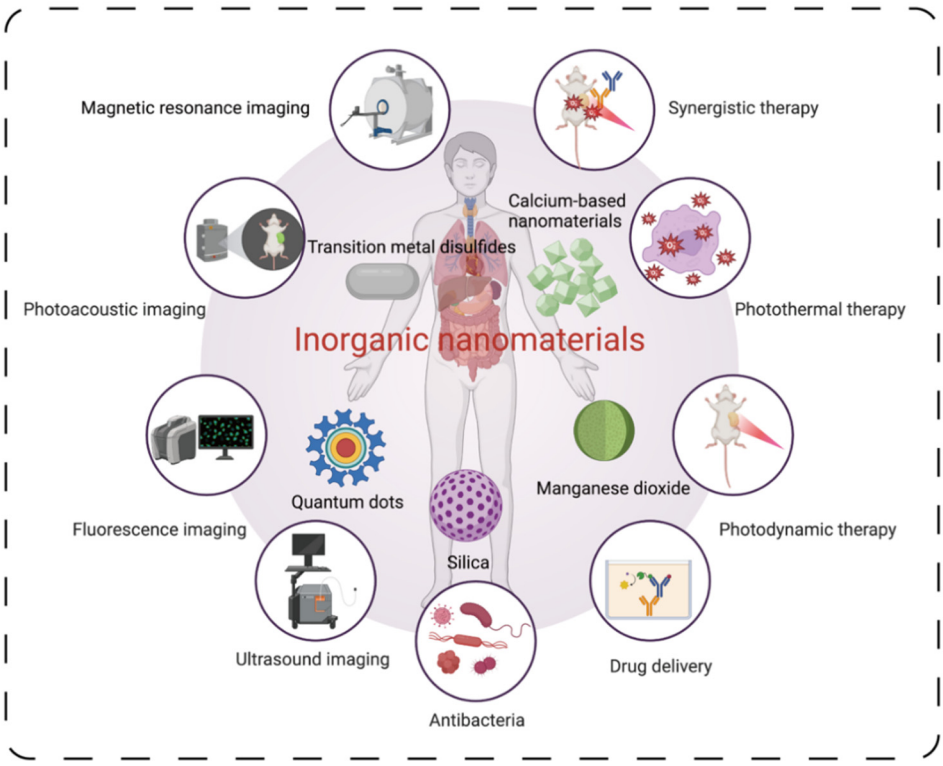

Figure 1. Schematic diagram of inorganic nanomaterials classification and biomedical applications.

2. Categorization and Characteristics of Inorganic Nanomaterials

Inorganic nanomaterials comprise a diverse spectrum of nanoscale materials, harnessed in medical applications to capitalize on their distinctive physicochemical properties, thereby augmenting therapeutic efficacy and diagnostic capabilities. These materials, typically composed of metal nanomaterials and non-metallic nanomaterials, can be meticulously engineered to manifest specific attributes tailored for a multitude of medical objectives. Here, we focus on the degradation and elimination properties of inorganic nanomaterials to assess their safety, optimize their use in applications, and evaluate their biocompatibility and toxicity for safe biomedical use.

2.1. Metal Nanomaterials

Metal, metal oxide, and other metal-related nanoparticles have been synthesized and utilized for therapeutic and diagnostic purposes, necessitating evaluation of their biodegradation and clearance pathways [22,23]. Traditional metal-containing nanomaterials, such as gold nanoparticles and magnetic metal oxides, show great potential in the field of medicine, especially in the diagnosis and treatment of cancer. Gold nanoparticles, renowned for their superior biocompatibility and ease of functionalization, have been extensively investigated for bioimaging and drug delivery applications. These nanoparticles are cleared via the hepatobiliary system, while magnetic metal oxide nanoparticles, such as iron oxide, are predominantly excreted through the kidneys. Currently, emerging metal nanoparticles have attracted the attention of researchers such as manganese dioxide (MnO_2), calcium-based nanomaterials and transition metal disulfides (TMDs).

2.1.1. Manganese Dioxide

MnO_2 nanomaterials, known for their good biocompatibility and biodegradability, can degrade in the TME to release manganese ions, enhancing MRI while also alleviating tumor hypoxia through oxygen generation. Furthermore, MnO_2 can be entirely decomposed and swiftly excreted via the kidneys, thereby mitigating the risk of long-term toxicity [24,25]. For example, Chen et al. developed a smart diagnostic 2D MnO_2 nanosheet for pH-responsive T_1 MRI imaging and controlled drug release, which can decompose and release drugs in mildly acidic environments. Meanwhile, its decomposed Mn^{2+} ions are biocompatible to be used in T_1 MRI imaging, which improves drug delivery efficiency and imaging accuracy [26]. Chen et al. prepared a multifunctional pH/H_2O_2-responsive human serum albumin (HSA)-encapsulated MnO_2 nanoparticles formed under alkaline conditions by biomineralization of Mn^{2+} ions from HSA. This system integrates a photosensitizer and a cisplatin prodrug, leveraging MnO_2 nanoparticles to react with H_2O_2 in the TME to generate oxygen, thereby enhancing PDT efficacy. Simultaneously, it decomposes into ultrasmall HSA-drug complexes to increase intratumor penetration [27].

2.1.2. Calcium-Based Nanomaterials

Calcium-based nanomaterials, such as calcium carbonate ($CaCO_3$) and calcium phosphate (CaP), exhibit potential applications in the biomedical field due to their high biocompatibility, biodegradability, and sensitivity to pH changes. $CaCO_3$ is stable under neutral pH conditions but dissociates into calcium ions and carbon dioxide in acidic environments, making it suitable for pH-responsive drug or gene delivery systems, particularly in tumor therapy where the acidic characteristics of the TME can be leveraged for precise release. Dong et al. developed monodisperse $CaCO_3$ nanoparticles as intelligent nanocarriers, which can rapidly decompose and release drugs under acidic conditions (Figure 2A). These nanoparticles exhibit pH-dependent T_1 magnetic resonance signal enhancement and fluorescence recovery, significantly increasing singlet oxygen production [28] CaP nanomaterials are considered ideal carriers for anticancer drugs or small interfering RNA (siRNA) due to their biodegradability and pH-responsiveness. The rigid framework of these nanomaterials allows for the loading of various types of drug molecules and prevents early leakage of drugs under neutral pH conditions (such as pH ≈ 7.4 in the blood circulation). Only upon reaching the acidic environment of tumor tissues do CaP nanomaterials release encapsulated calcium and phosphate ions, thereby releasing the drug. This property makes CaP nanoparticles highly advantageous in drug delivery systems, enabling precise release of therapeutic agents at the right time and location, enhancing treatment efficacy while minimizing potential damage to normal cells [29] (Figure 2B).

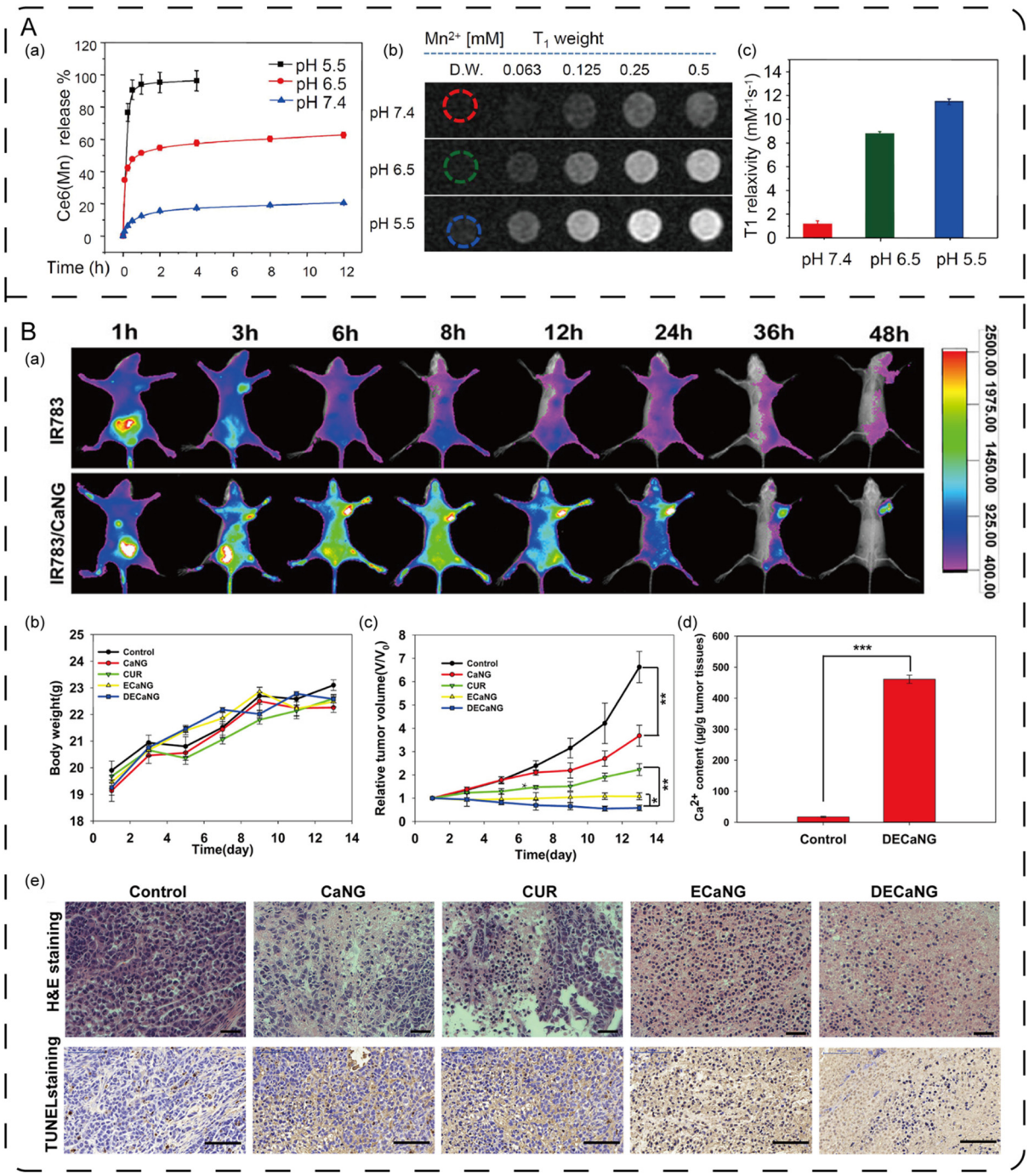

Figure 2. Biological properties of metal nanomaterials. (A) Enhancement of MRI triggered by pH. (a) Time-dependent release of $Ce_6(Mn)@CaCO_3$- polyethylene glycol (PEG) from phosphate buffered saline (PBS) solutions at different pH values. (b) T_1-weighted MRI images with different concentrations of $Ce_6(Mn)@CaCO_3$-PEG in; m PBS at different pH values after incubation for 4 hours. (c) T_1 relaxation at different pH was statistically analyzed in Figure A(b) [28]. Copyright 2016, Elsevier Ltd. (B) In *vivo* distribution and efficacy assessment in mice. (a) In *vivo* distribution at different time points after intravenous injection of IR783 and IR783/CaNG. (b) Changes in body weight of mice after different treatments (n=5). (c) Relative changes in tumor volume in mice after different treatments (n = 5). (d) Ca^{2+} levels in DECaNG-treated tumor tissues (n = 3). (e) Tumor tissues were stained with H&E staining and terminal deoxynucleotidyl transferase mediated dUTP nick-end labeling (TUNEL) staining after different treatments. Scale bar: 25 μm for H&E staining and 100 μm for TUNEL staining [29] Copyright 2018, American Chemical Society.

2.1.3. Transition Metal Disulfides

TMDs, a class of two-dimensional materials composed of transition metals (e.g., molybdenum Mo, tungsten W) and sulfur-group elements (e.g., sulfur S, selenium Se, tellurium Te), show remarkable potential for nanomedicine applications due to their unique physicochemical properties. The biodistribution, toxicological properties and metabolic pathways of these materials are the focus of current research to ensure their safety and efficacy [30]. The low toxicity and rapid excretion properties of TMDs make them ideal candidates for drug delivery systems. They can be used as drug carriers to achieve targeted release of drugs and precision therapy with the assistance of imaging technology. For instance, Zhou et al. successfully synthesized multifunctional ultrasmall copper sulfide nanodots (CuS NDs) with hydrodynamic diameters of less than 6 nm through a polyvinylpyrrolidone-assisted chemical reaction. These nanodots can be radiolabeled with the copper-64 radioisotope for positron emission tomography (PET) imaging. The CuS NDs exhibited rapid excretion in vivo, with approximately 95% of the nanodots cleared through the urinary system within one day, leaving minimal residue in the liver and spleen. Additionally, they demonstrated excellent performance in PTT, effectively inhibiting tumor growth [31]. Zhang et al. investigated a $MoTe_2$-based nanosheet, designed as a multifunctional cancer therapy platform. These nanosheets exhibit excellent stability under normal physiological conditions within the body. However, upon exposure to NIR laser irradiation, they can rapidly degrade and be cleared via biological processes. This characteristic helps to reduce potential toxicity from long-term accumulation in the body [32]. Recently, researchers have constructed a bioabsorbable silicon-based neurochemical analysis system by combining two-dimensional transition metal disulfides (2D TMDs, such as MoS_2 and WS_2) with catalytic iron nanoparticles (Fe NPs). 2D TMDs have become the core material of this system due to their mechanical flexibility, high conductivity, catalytic activity and controllable chemical properties. Studies have shown that the heterostructure of 2D TMDs and Fe NPs can efficiently detect DA through electrostatic interactions and catalytic oxidation, while showing high sensitivity, selectivity and reversibility. In addition, 2D TMDs gradually degrade in a physiological environment, reducing the risk of postoperative complications [33]. Through experiments and theoretical simulations, the study revealed the chemical response mechanism and degradation characteristics of 2D TMDs, demonstrating their potential clinical application value in the diagnosis and treatment of neurodegenerative diseases.

2.2. Non-Metallic Nanomaterials

QDs and silica nanomaterials in non-metallic oxides have shown wide application potential in biomedicine, energy, catalysis and other fields due to their unique physical and chemical properties. QDs achieve adjustable optical properties through size regulation, while silica nanomaterials achieve multifunctional integration through pore structure and surface modification. With the continuous development of nanotechnology, these materials will play an important role in more fields and provide strong support for scientific and technological innovation and human health.

2.2.1. Quantum Dots

2.2.1.1. Carbon-Based Quantum Dots

In contrast to traditional semiconductor QDs, carbon dots (CDs) are emerging as novel fluorescent markers, offering enhanced modifiability, improved solubility, and reduced toxicity [34,35]. It is noted that CDs meet the basic requirements for clinical use, including fast excretion rate, low toxicity, and the ability to provide a stable light signal. Leveraging these attributes, diverse types of CDs have been extensively integrated into phototherapy, employed as contrast-enhancing agents for imaging, and synergistically combined with therapeutic agents to formulate comprehensive treatment strategies [36,37]. In vivo studies have demonstrated that CDs exhibit excellent biocompatibility and non-toxicity, with rapid clearance from mice following various injection routes, including intravenous, subcutaneous, and intramuscular administration [38]. The surface charge of CDs markedly influences their biodistribution and clearance pathways, with positively charged particles preferentially absorbed by the liver, whereas neutral or negatively charged particles predominantly excreted via the kidneys. The mode of injection also affects the clearance efficiency of CDs, e.g., CDs are cleared faster when administered intravenously [39]. CDs and graphene quantum dots (GQDs) have been widely investigated for biomedical applications due to their excellent water solubility, biocompatibility and photostability [40,41]. CDs can serve as photoacoustic (PA) contrast agents and NIR photothermal agents, with their biodegradability and renal excretion verified through whole-body PA imaging and degradation experiments [42]. GQDs, known for their strong fluorescence and high quantum yield, are utilized in bioimaging and drug delivery systems. Research indicates that following intravenous administration, GQDs predominantly accumulate in the kidneys and tumors, and PEG modification can amplify

their accumulation via the enhanced permeability and retention (EPR) effect [43] (Figure 3A). Yan et al. proposed an innovative method to enhance the capabilities of tumor imaging and long - term visualization of local pharmacokinetics by implanting GQDs into PEG-ylated nanoparticles. These implanted GQDs showed longer blood circulation time and higher tumor accumulation in vivo than typical GQDs, with more than 4-fold prolongation of blood circulation and 7–8-fold increase in tumor accumulation. The preparation of this nanocomposite was achieved through a bottom-up molecular approach, in which small-molecule pyrene grew in-situ in the PEG layer to form GQDs. In addition, due to the presence of the PEG layer, these nanoparticles showed significant advantages in terms of metabolism and clearance in living organisms, including reduced clearance by the immune system and enhanced tumor accumulatio n. These properties make the implanted GQDs an ideal tool for multi-modal molecular imaging and real-time monitoring of the dynamic changes of nanoparticles in the TME [44] (Figure 3B).

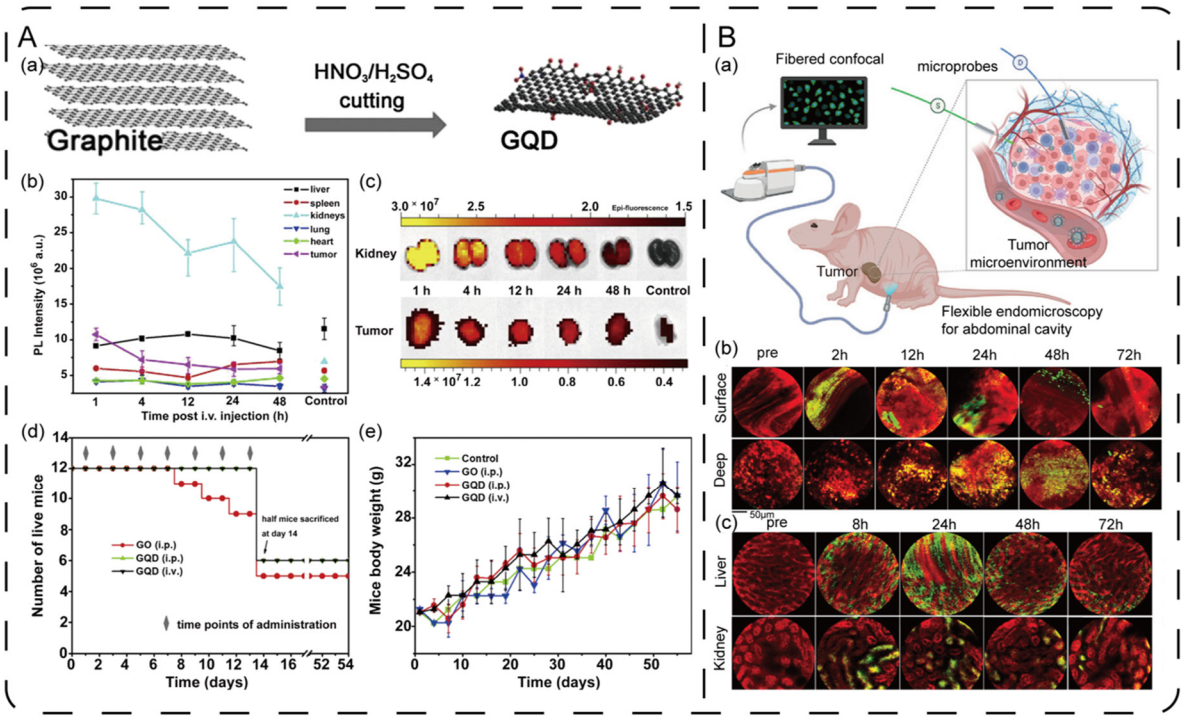

Figure 3. Biological properties of GQDs. (A) In vivo toxicity studies of GQDs. (a) Synthesis of GQD obtained by oxidation of graphite. (b) PL intensity indicates the concentration of GQD in major organs and tumors of mice after intravenous injection of GQD-PEG-cy7. (c) Changes in GQD concentrations in kidneys and tumors under NIR irradiation. (d) Survival curves of mice after 7 injections of GQD-PEG and GO-PEG, respectively. (e) Graph of body weight changes in surviving mice [43]. Copyright 2014, Elsevier Ltd. (B) Long-term surveillance of NPC-GQDs-PEG in tumor tissues. (a) Schematic illustration of the fibered confocal fluorescence microscopy (FCFM) for the imaging of tumor tissues and major organs. (b) Accumulation, diffusion and biodistribution of the probes in tumor tissues were monitored using FCFM. Red: EB, green: NPC-GQDs-PEG/2-DG. (c) Biological distribution and metabolism of the probes in the liver and kidney were monitored using FCFM [44]. Copyright 2023, Wiley-VCHGmbH.

2.2.1.2. Cadmium-Based Quantum Dots

QDs are primarily utilized in the biomedical field for imaging and sensing applications, owing to their high brightness, tunable emission wavelengths, and sensitivity to environmental changes [45]. Researchers commonly utilize CdS, CdSe, and CdTe/CdSe core/shell QDs, often encapsulated with ZnS or ZnSe as protective shells [46]. Through meticulous optimization of liquid-phase synthesis techniques and reaction conditions, QDs tailored for bio-imaging and therapeutic purposes are synthesized. Frangioni and collaborators described the study of DL-cysteine-coated CdSe (ZnCdS) quantum dots (QD-Cys) in in vivo applications. QD-Cys has an ultra-small size (hydrodynamic diameter of 5.9 nm), which is close to or below the renal clearance threshold, and can be quickly cleared through the kidneys within 4 hours, reducing long-term retention in the body, thereby significantly reducing the risk of toxicity. In addition, cysteine coating makes the surface of QDs charge neutral at physiological pH, avoiding nonspecific binding with serum proteins and improving the biocompatibility and stability of the

material. These characteristics ensure the in vivo safety of QD-Cys [47]. Recent studies have discussed the safety and versatility of HSA functionalized CdTe quantum dots (CdTe-HSA QDs) in biomedical applications. CdTe-HSA QDs are surface modified with HSA, which has small size (1–5 nm), high water solubility and good biocompatibility, significantly reducing the release and potential toxicity of Cd^{2+} ions. Experiments have shown that CdTe-HSA QDs are stable and non-aggregating in serum, have low toxicity to normal cells (such as HEK-293), but show certain anticancer activity against HeLa cells [48]. Rao et al. reported the use of amorphous silicon dioxide as a surface coating for QDs, which prevents the release of quantum dot components into the physiological environment and thus improves their biocompatibility. Silica-coated CdTe QDs demonstrated superior renal clearance rates relative to commercially available QD605, coupled with minimal uptake in the liver and spleen and extended circulation times [49].

2.2.1.3. Silicon Quantum Dots

Silicon quantum dots (Si QDs) are zero-dimensional nanomaterials with several advantages, including abundant natural reserves, low cost, low toxicity and good biocompatibility. Silicon is abundant in the earth's crust, easily extracted, and naturally occurs in living organisms in the form of orthosilicates, which are easily excreted in urine [50]. Ultra-small Si QDs have garnered FDA approval for human clinical trials [51–53]. Owing to these distinctive attributes, Si QDs are regarded as compelling alternatives to metal-based semiconductor quantum dots and hold significant promise for applications in bioimaging, disease diagnostics, and therapeutic interventions. Si-QDs can be combined with magnetic nanoparticles to form biocompatible magnetic-fluorescent nanoprobes. These advanced probes seamlessly merge the optical properties of Si-QDs with the superparamagnetic attributes of iron oxide nanoparticles, facilitating enhanced cellular uptake and illuminating the luminescence stability within the microenvironment of prostate cancer tumor models. This innovation provides a novel nanoplatform for multimodal imaging and delivery applications [54]. Hanada, Sanshiro et al. synthesized water-soluble aminoprofen-conjugated Si-QDs (Ap-Si), and the results showed that the "silicon drug" had lower toxicity than the control Si-QD and the original drug, indicating that the surface integration of ligand/receptor-type drugs might reduce adverse interactions between cells and drug molecules. Additionally, Si-QDs maintained the pharmacological efficacy of the original drug (inhibiting the COX-2 enzyme), with the drug effect correlating with the integration ratio of the original drug, potentially controlling the binding interactions between COX-2 and the silicon drug [55]. The unique properties of Si-QDs provide new tools and methods for biomedical research and clinical diagnosis.

2.2.2. Silica

Silica nanomaterials are versatile nanomaterials with diverse morphologies and sizes. They possess abundant surface chemical properties, including silica hydroxyl groups, which can be chemically modified to improve their compatibility in different media. These nanomaterials exhibit good biocompatibility and degradability, giving them potential for biomedical applications such as drug carriers. The degradation and elimination of silica nanomaterials are influenced by various factors, including their size, morphology, surface functionalization and surface charge. It was shown that colloidal mesoporous silica nanoparticles and uniform mesoporous silica nanoparticles with different particle sizes showed similar degradation rates in simulated body fluids, which were related to their surface area [56,57]. He et al. study revealed that high concentrations and low surface area of mesoporous silica nanoparticles (MSN) lead to reduced degradation percentages and extended degradation times [58]. The shape of nanoparticles also determines their in vivo kinetics and clearance rates, with spherical particles degrading faster than rod-shaped particles [59–61]. In vivo distribution and excretion studies underscore that PEG modification can mitigate nanoparticle accumulation in the liver, spleen, and lungs, thereby extending the circulation half-life and impacting their biodegradation and excretion pathways [62]. Bein and collaborators engineered colloidal core-shell mesoporous silica with varying PEG chain lengths, revealing that the PEG shell curtailed the degradation rate of silica nanoparticles in simulated body fluid. This effect was primarily attributed to the hydrophilicity of PEG, which inhibits protein adsorption and diminishes unfavorable interactions. Nanoparticles modified with long and dense PEG chains exhibited even slower degradation [63].

Additionally, different surface modifications may influence the degradation and clearance of nanomaterials. He et al. synthesized three types of surface-modified silica nanoparticles (OH–SiNPs, COOH–SiNPs, and PEG–SiNPs), finding that all nanoparticles could be partially cleared through the renal excretion pathway, but PEG–SiNPs exhibited a longer circulation time and lower liver uptake [64] (Figure 4A). Lin's team synthesized a multifunctional MRI contrast agent based on MSN that is rapidly eliminated through the kidneys after imaging. The nanoprobe contains Gd chelate units that covalently bind to the MSN via redox-responsive junctions and is functionalized with PEG and anisamide ligands to enhance biocompatibility and targeting. Anisamide targets the

sigma receptor that is overexpressed in a variety of epithelial cancer cells. In vitro experiments demonstrated its effectiveness and targeting ability, and in vivo experiments showed that the Gd chelator unit was rapidly cleaved by blood pool thiols and the Gd complex was rapidly excreted through the kidneys [65] (Figure 4B). The interaction of the surface charge of nanoparticles with serum proteins affected their biodistribution, with highly positively charged MSNs showing faster hepatobiliary excretion. By modulating the surface charge, the residence time of nanoparticles within the body can be altered, thereby influencing their excretion pathways. Souris et al. synthesized highly positively charged, NIR MSN for high-volume traceable drug delivery (Figure 4C). Upon binding of MSN to NIR fluorescent dyes, the more charged ones with a charge of +34.4 mV at pH 7.4 are rapidly excreted from the liver to the gastrointestinal tract, and the less charged ones with a charge of −17.6 mV at pH 7.4 are isolated in the liver, suggesting that the charge-dependent adsorption of serum proteins promotes the hepatobiliary excretion of silica nanoparticles and that the residence time of the nanoparticles in vivo can be controlled by regulating the surface charge [66]. These findings are crucial for understanding and further controlling the transport of nanoparticles in biomedical applications.

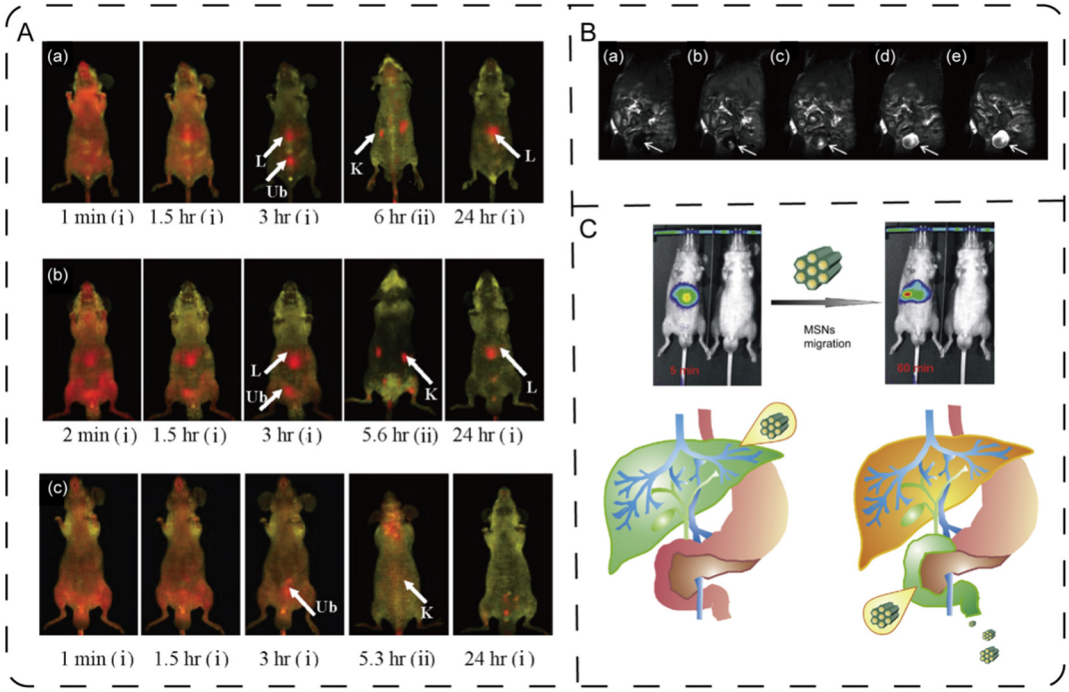

Figure 4. Biological properties of silica nanomaterials. (A) In *vivo* distribution of SiNPs with different surface modifications at different time points after injection. ((a) – (c), (i), abdominal imaging; (ii), dorsal imaging). (a) OH-SiNPs; (b) COOH-SiNPs; (c) PEG-SiNPs. Arrows mark the locations of kidneys (K), liver (L), and bladder (Ub) [64]. Copyright 2008, American Chemical Society. (B) MRI images of nude mice injected intravenously with PEG-Gd-MSN (0.080 mmol kg $^{-1}$ Gd dose) for 0 min (a), 5 min (b), 15 min (c), 30 min (d), and 45 min (e), focused on the bladder (white arrow) [65]. Copyright 2011, WILEY-VCH Verlag GmbH & Co. KGaA, Weinheim. (C)MSN distribution in *vivo* [66]. Copyright 2010, Elsevier Ltd.

3. Application of Inorganic Nanomaterials in Disease

Inorganic nanomaterials have emerged as a novel platform in disease therapeutics due to their unique physicochemical properties, such as excellent optical, thermal, and magnetic properties, as well as their superior ability in bioimaging, antibacteria and therapy.

3.1. Bioimaging

Precision in tumor imaging is paramount for early tumor detection and for providing imaging guidance during surgical interventions. In contrast to organic molecules, inorganic nanomaterials have emerged as pivotal materials for the development of nanoprobes in tumor imaging, owing to their distinctive physical and chemical attributes, including superior magnetic properties, X-ray attenuation capabilities, and optical characteristics. Notably, inorganic nanomaterials endowed with bioactivity can react to the biochemical milieu within tumors, such as variations in pH levels, alterations in redox conditions, and the overexpression of enzymes in tumor cells,

facilitating stimulus-responsive imaging. These bioactive inorganic nanoprobes enhance imaging signals and elevate the sensitivity and target-to-background ratio when subjected to specific biochemical triggers within tumors. Moreover, the majority of these probes are characterized by their favorable biodegradability, which markedly diminishes their potential toxicity in comparison to conventional inorganic nanoprobes. Consequently, the development of activatable inorganic nanoprobes that can respond to the specific biochemical environment of tumors is of profound importance for advancing the clinical application and regulatory approval of inorganic nanomaterials. In this section, we will explore the multifaceted applications of inorganic nanomaterials within the realm of tumor imaging, ranging from MRI to PAI, FLI, and ultrasound imaging (USI).

3.1.1. Magnetic Resonance Imaging

MRI renowned for its superior spatial resolution and sensitivity, has found extensive application in clinical settings. Inorganic nanomaterials, functioning as activatable MRI probes, have the capability to modulate T_1 and T_2 relaxation signals upon exposure to endogenous stimuli, thereby markedly elevating the sensitivity and precision of tumor imaging. This advancement offers robust support for achieving accurate diagnosis and effective monitoring of therapeutic interventions. Currently, despite the widespread application of superparamagnetic Fe_3O_4 nanoparticles—which boast high magnetization and commendable biosecurity—as magnetic resonance contrast agents for tumor imaging, the precision of tumor diagnosis continues to be compromised by the absence of tumor-specific targeting and the confounding signals from normal tissues. Glutathione (GSH) is a tripeptide composed of glutamic acid, cysteine and glycine. It plays a vital role in the cell's antioxidant defense system, helping to protect against oxidative stress and maintain cellular redox balance. Taking advantage of the overexpression of GSH in tumors, Wang et al. developed an ultrasmall Fe_3O_4 assembly that functions as an endogenous GSH-responsive MRI contrast agent. This innovative agent is synthesized by bonding ultrasmall superparamagnetic Fe_3O_4 with a crosslinking agent, cystamine, to create Fe_3O_4 nanoclusters that demonstrate T_2 imaging capabilities. Once introduced into tumor tissue, the disulfide bonds within cystamine are selectively cleaved by GSH, leading to the disassembly of the Fe_3O_4 nanoclusters into ultrasmall Fe_3O_4 nanoparticles. This disassembly process results in a shift from T_2 to T_1 relaxation signals, significantly enhancing the accuracy of tumor diagnosis [67]. Guan et al. have engineered a ternary alloy PtWMn nanocube, serving as a sophisticated reservoir and release mechanism for manganese ions (Figure 5A). By crafting a microenvironment-responsive nanoplatform, this system adeptly modulates the manganese ion release within the TME, thereby boosting ROS production, oxygen generation, glutathione depletion, and synergistically amplifying iron's biological impact. Furthermore, this nanoplatform exhibits responsiveness in high-field MRI, allowing for the real-time tracking of manganese ion release and iron mutation initiation via T_1/T_2-MRI signal alterations. This innovation offers a cutting-edge nanomedicine delivery and monitoring approach for precision iron poisoning therapy under MRI guidance [68]. Inorganic nanomaterials selectively augment the sensitivity of MRI to specific biomarkers, thereby elevating the imaging contrast of the TME. This innovative approach not only facilitates more precise tumor diagnosis but also holds the potential for extensive clinical adoption in the foreseeable future.

3.1.2. Photoacoustic Imaging

PAI technology synergistically combines the advantages of optics and acoustics, paving the way for high-resolution molecular imaging. Within the realm of bioactive inorganic nanomaterials, activatable PA contrast agents are particularly noteworthy. Their ability to precisely respond to target-specific changes renders them highly effective in elevating the sensitivity and specificity of tumor detection [69]. Zeng et al. engineered a pH-sensitive Fe (III)-GA nanoparticle that exhibits easy degradation under neutral conditions yet remains stable in acidic environments. This unique property enables the nanoparticle to be selectively retained at tumor sites while facilitating its metabolism in other organs, thereby delivering exceptional in vivo PAI and photothermal therapeutic outcomes [70]. Wang et al. successfully prepared TME-activated Fe/Cu co-doped polyaniline (Fe-Cu@PANI) nanoparticles, in which Cu (II) reacts with GSH present in tumors, leading to a red shift in the absorption spectrum of the Fe-Cu@PANI nanoparticles and simultaneously triggering precise PAI of tumors and effective PTT [71] (Figure 5B). Zhang et al. innovatively crafted a H_2S-activated copper-based metal-organic framework (Cu-MOF) as a NIR ratiometric PA probe for real-time assessment of hydrogen sulfide (H_2S) levels within living organisms. Since the level of H_2S in colorectal cancer is significantly higher than that in normal tissues, this probe generates copper through the in situ reaction of Cu-MOF with endogenous H_2S, which enables the monitoring of H_2S levels and in situ colorectal cancer imaging. The synthesized Cu-MOF demonstrates exceptional PA reactivity, characterized by high selectivity and rapid kinetics towards H_2S derived from tumors, underscoring its critical role in elucidating the etiology and progression of colorectal cancer [72]. Exploring

biomarkers for activatable PA probes presents a promising avenue in the field of cancer diagnosis and treatment. Leveraging PAI-based bioactive inorganic nanomaterials, which possess the ability to specifically identify diseased tissues from healthy ones, can mitigate side effects and toxicity, thereby facilitating real-time tumor surveillance and precise prognostication. Future research should concentrate on PAI-guided therapy, surgery, and drug activation, developing novel activatable inorganic nanomaterial PA probes to elucidate cancer biological mechanisms and enhance clinical detection and treatment efficiency [69].

3.1.3. Fluorescence Imaging

FLI is superior to other imaging techniques due to its high sensitivity and resolution, by selectively activating the imaging agents in accordance with the distinct characteristics of tumors versus normal tissues, the tumor-to-background ratio (TBR) can be markedly enhanced. This enhancement not only elevates the sensitivity and contrast of FLI but also expedites its transition to clinical practice [73]. Compared with continuously activated contrast agents, inorganic nanoprobes remain non-fluorescent until the activation of tumor-specific molecules, which further enhances the TBR and provides information on tumor-associated molecules. MnO_2 nanoparticles are biodegradable bioactive inorganic nanomaterials that achieve fluorescence quenching by surface modification of fluorescent probes and utilizing the fluorescence resonance energy transfer (FRET) effect. In normal tissues, the fluorescence signal is undetectable, the fluorescence signal is restored due to the decomposition of MnO_2 by GSH, H_2O_2, and acidic conditions in the TME. This distinctive property facilitates tumor-specific FLI, significantly enhancing the imaging's specificity and sensitivity [74]. Yao et al. developed a novel therapeutic nanoprobe that utilizes a multifunctional DNA-templated silver nanocluster (AgNC)/porphyrin/MnO_2 nanoplatform for unlabeled Zn^{2+} FLI. The intracellular degradation of MnO_2 nanosheets by GSH, H^+, and H_2O_2 results in the release of AgNCs, which dynamically self-assemble via a three-way DNA junction structure to facilitate label-free FLI of Zn^{2+} within cells [75]. Wei et al. designed a novel nanoprobe VGd@ICG-FA for improving the radiotherapy effect and precision surgery of breast cancer. The probe achieves efficient targeting through Gd coating and folic acid modification, and uses glutathione depletion and NIR second-zone FLI to enhance the sensitivity of cancer cells to radiotherapy, and navigates to accurately locate microcancers during surgery, with the advantage of no systemic side effects [76]. Recently, researchers have developed a new nanoprobe PCN@FL that can simultaneously detect and image hypochlorous acid and phosphorylation levels in early atherosclerosis, providing a new tool for early diagnosis and mechanism research of the disease (Figure 5C). Experimental results showed that hypochlorous acid and phosphorylation levels in the serum of early-stage atherosclerotic mice were significantly higher than those of normal mice, verifying the potential of this nanoprobe in disease assessment [77].

3.1.4. Ultrasound imaging

USI has become an important technique for clinical tumor detection and tissue biopsy due to its low cost, real-time performance, non-ionization and deep tissue penetration. Fluorocarbon microbubbles are used as USI contrast agents to improve ultrasound therapy through the cavitation effect, but their large volume, poor stability, and short cavitation activity limit their application in tumor imaging and therapy [78]. Novel inorganic nanomaterial-based ultrasound contrast agents, owing to their superior stability and tumor specificity, present fresh prospects for tumor imaging and therapy. Furthermore, the acid-induced degradation characteristics of $CaCO_3$ open up new avenues for contrast-enhanced USI, facilitating enhanced assessment of organ function and physiological information. For example, Feng et al. developed a pH/ultrasound dual-responsive mesoporous $CaCO_3$ nanoparticles loaded with the acoustic sensitizer HMME and modified surface HA, which can precisely target tumors in the tumor-acidic environment and ultrasound, leading to cell necrosis and vascular disruption through CO_2 generation and cavitation effects. Additionally, they function as ultrasound contrast agents, enhancing the detection and identification of malignant lesions [79]. Inorganic contrast agents such as silica nanoparticles and gold nanoparticles offer reliable carriers for activatable ultrasound contrast agents due to their stability. Hollow mesoporous organosilica nanoparticles, engineered with glutathione-responsive biodegradable linkages through disulfide bonds, are meticulously loaded with indocyanine green (ICG) and perfluoropentane These innovative nanoparticles are designed to deliver a dual-action approach, combining PTT with USI, specifically tailored for the intricate landscape of the TME [80]. In an intriguing study, Meng et al. developed a BiF_3@PDA@PEG (BPP) nanoparticles with good monodispersity and core-shell structure by initially forming BiF_3 nanoparticles through coprecipitation, coating with polydopamine (PDA), and then modifying with PEG, which undergoes self-aggregation at acidic pH via a hydrophilic to hydrophobic transition of BPP, increasing tumor density and acoustic

impedance aberration (Figure 5D). This enhancement in turn boosts the sensitivity of USI for acidic tumor tissues, providing a novel strategy for the development of activatable USI inorganic nanomaterials [81].

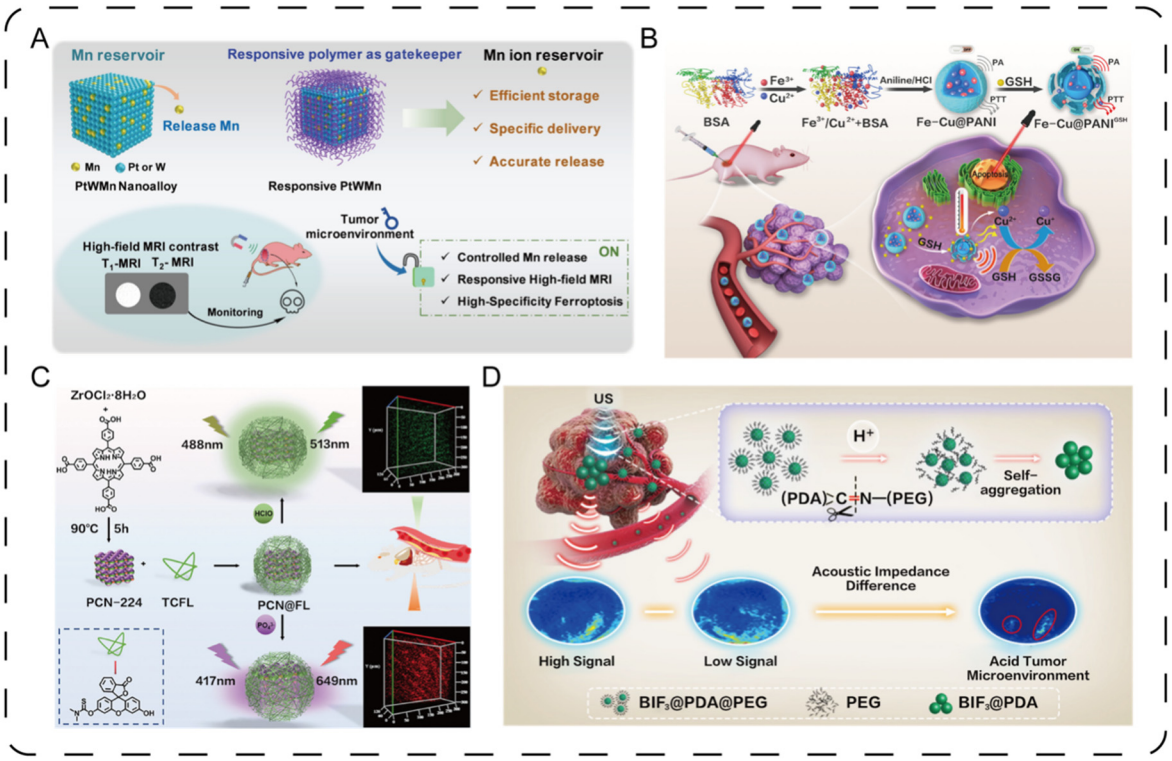

Figure 5. Applications of inorganic nanomaterials in bioimaging. (A) pH-responsive R-PtWMn nanoplatforms for manganese storage in high-field MRI monitoring and TME-induced iron death [68]. Copyright 2022, Wiley-VCH GmbH. (B) Preparation of Fe-Cu@PANI nanoparticles and their activation mechanism in PAI and tumor PTT [71]. Copyright 2021, The American Association for the Advancement of Science. (C) Synthesis of PCN@FL and its application in the detection and imaging of phosphorylation and HClO levels in early AS models [77]. Copyright 2023, Wiley-VCH GmbH. (D) BPP as a mechanism for sensitive diagnosis of acidic TME by smart nano-UCA [81]. Copyright 2022, American Chemical Society.

3.2. Antibacteria

At the beginning of the 20th century, infectious diseases were reigned as the predominant cause of global mortality, and the invention of antibiotics and other antimicrobial agents significantly reduced their morbidity and mortality rates, but faced challenges such as high price, toxicity, and drug resistance [82,83]. Inorganic nanomaterials show great potential in antimicrobial therapy due to their unique physical and chemical properties. Through meticulous design of specific shapes and sizes, functionalization to target specific bacterial species, and synergistic integration with modalities such as PDT and PTT, these nanomaterials function as potent antibacterial agents or carriers. This strategic approach not only amplifies antibacterial efficacy but also mitigates the risk of toxicity to normal cells, positioning them as a promising frontier in the battle against bacterial infections [84 – 86]. Chronic obstructive pulmonary disease (COPD) is a condition characterized by airflow obstruction due to chronic inflammation, with patients being highly susceptible to infections due to compromised immune function, leading to exacerbated symptoms and high mortality rates [87,88]. Amikacin (AM) is the main drug used for the treatment of COPD, but intravenous administration suffers from low bioavailability and high toxicity. Yu et al. developed a novel drug delivery system, combining PEG-modified chitosan (CS) nanoparticles and black phosphorus quantum dots (BPQDs) to co-deliver AM for COPD treatment. This system promotes the dissolution of CS and release of AM through the acidic environment generated by the decomposition of BPQDs. NPs dissolution and AM release, which enhanced the antimicrobial properties and effectively inhibited biofilm formation. In vivo studies demonstrate that the system exhibits excellent mucus penetration and antibacterial capabilities, offering potential clinical applications for COPD treatment [89].

In the field- of antimicrobial therapeutics, researchers are exploring the use of smart inorganic nanomaterials to mimic the activity of horseradish peroxidase (HRP), which are capable of generating ROS through Fenton or

Fenton-like reactions to destroy bacteria [90]. However, using these nanoenzymes alone may not completely eliminate bacteria [91]. To bolster antibacterial efficacy, investigators have proposed combining nanozymes with PTT, leveraging the photothermal effect to elevate temperatures and accelerate reaction rates, thereby augmenting antibacterial effects [90]. Currently, a variety of nanoenzymes, such as carbon nanoparticles [92], metal or bimetallic oxides [93,94], and single-atom nanoenzymes [92], have been used to enhance the antibiotic effect of PTT in order to address the problem of antibiotic resistance. However, relying solely on these nanozymes may not completely eradicate bacteria. Wang et al. developed a nickel disulfide nanozyme that effectively disinfects *E. coli* and methicillin-resistant staphylococcus aureus through biodegradation, GSH depletion, enhanced PTT, and Fenton-like catalytic activity. It also possesses excellent photothermal performance and biodegradability, offering a highly efficient and safe strategy for antibacterial treatment [95]. Recently, inspired by the structure of vitamin U, researchers have carefully designed and synthesized a series of sulfonium peptides with different degrees of alkylation. These peptides show excellent performance in antibacterial activity, hemolysis rate and cytotoxicity, providing an important structural basis and theoretical basis for the development of new antibacterial drugs. As shown in Figure 6, by adjusting the degree of alkylation of the peptide, its antibacterial properties and biocompatibility can be precisely controlled, thereby achieving efficient killing of pathogens such as methicillin-resistant Staphylococcus aureus (MRSA) while minimizing damage to normal cells. This innovative peptide design strategy not only broadens the research field of antimicrobial peptides, but also provides a new solution to the increasingly severe problem of bacterial resistance [96]. Antibiotic resistance in microorganisms is a growing problem that threatens human health. To tackle this challenge, researchers are exploring the development of "nano-antibiotics" using inorganic nanomaterials. These nano-antibiotics are effective in combating infectious diseases by interacting with bacterial cell membranes, proteins, nuclei, mitochondria, or transmembrane electron transport systems to disrupt bacterial structures.

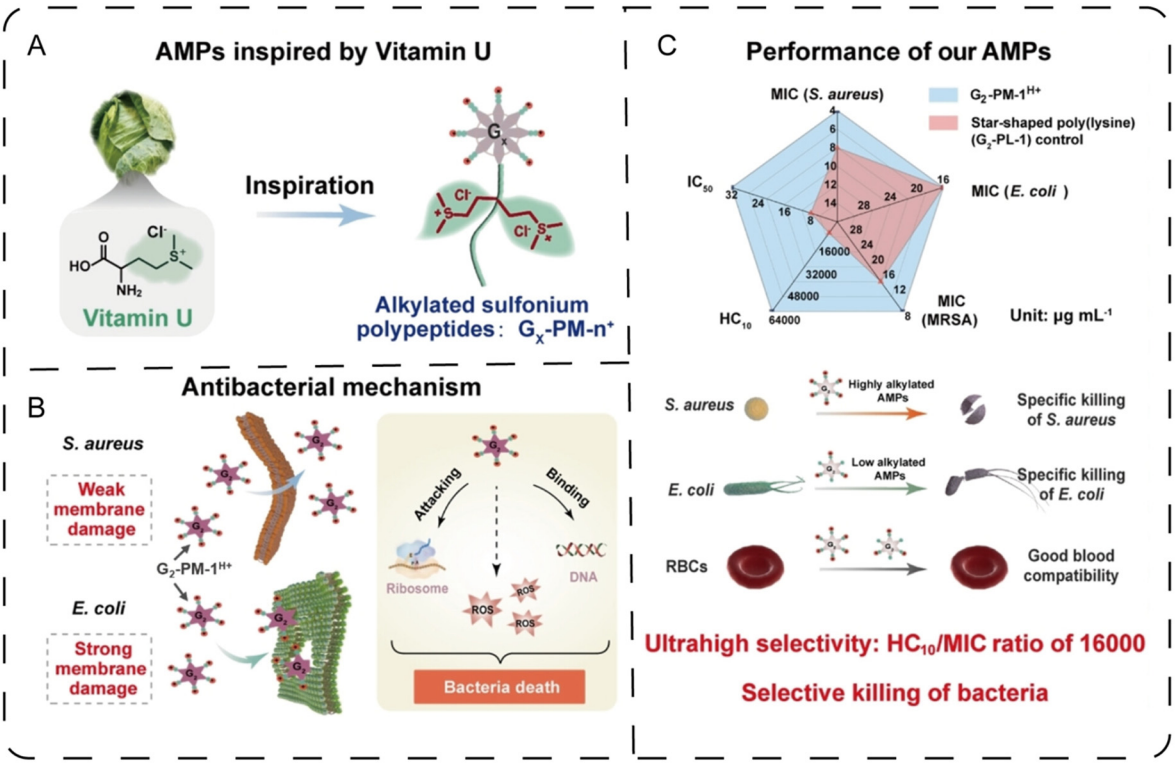

Figure 6. Antimicrobial principles and specificity of alkylated sulfonium peptides derived from vitamin U-inspired peptides. (A) Structurally inspired alkylated sulfonium polypeptides (Gx-PM-n+) of vitamin U. Gx represents polyamidoamine dendritic polymer (x = 0, 1 and 2 generations) triggers. (B) Antimicrobial principle of G2-PM-1H$^+$ versus Staphylococcus aureus and Escherichia coli. (C) Antibacterial activity, cytotoxicity and hemolysis of G2-PM-1H$^+$ and astro-polylysine (G2-PL-1) as controls [96]. Copyright 2023, Wiley-VCH GmbH.

3.3. Therapy

Inorganic nanomaterials have demonstrated extensive application potential in disease treatment. Through various means such as drug delivery, PDT, PTT, and synergistic therapy, these nanomaterials facilitate targeted

drug delivery, enhanced light absorption, efficient photothermal conversion, and multi-modal treatment strategies. This approach significantly improves therapeutic efficacy, reduces side effects, and facilitates personalized treatment.

3.3.1. Drug Delivery

To achieve safe and effective therapies, nanocarriers are used for drug delivery, and inorganic nanomaterials are ideal drug delivery platforms due to their ease of preparation, stability and biocompatibility. Over the past decade, mesoporous silica nanoparticles have become ideal for drug delivery systems due to their tailored mesoporous structure, large surface area, good biocompatibility and easy surface functionalization [97,98]. Yan et al. developed a multifunctional hybrid drug delivery system with a core-shell structure, which is based on silica-coated Fe_3O_4 nanospheres with an outer layer of ordered mesoporous silica and a phosphor (YVO_4:Eu^{3+} or $NaYF_4$: Yb, Er/Tm) deposited in the outermost layer. This structure endows the material with up- and down-conversion emission capabilities as well as high magnetization properties. Notably, by monitoring changes in photoluminescence intensity, the drug release process from the multifunctional carrier can be tracked and monitored in real time [99]. Iron oxide nanomaterials are promising for a wide range of applications in drug delivery due to their unique physicochemical properties such as targeting, magnetic guidance, controlled release systems, biocompatibility, and multifunctionality [100]. They are also one of the primary components among inorganic nanomedicines approved by the FDA [101]. The Ni team utilized magnetic iron oxide nanoparticles (MIONPs) as a multifunctional delivery platform, employing folic acid ligands to precisely target glioblastoma (GBM) while simultaneously delivering cisplatin and siRNA that inhibits GPX4, thereby achieving comprehensive therapy. The delivery of MIONPs not only enhances drug and gene silencing molecule targeting, but also offers the possibility of monitoring the therapeutic effects by MRI in the future [102]. As shown in Figure 7A (a), Li et al. designed an innovative nanocarrier for stroke treatment. This nanocarrier consists of a platelet membrane and γ-Fe2O3 magnetic nanoparticles (MNs) that can load l-arginine (PAMN). The platelet membrane has a natural thrombus-targeting adhesion ability, while the γ-Fe2O3 magnetic nanoparticles have a magnetic field response ability. These 200-nanometer-sized PAMNs are injected through the tail vein and can be precisely accumulated in the stroke lesion area under the guidance of an external electromagnetic field. Once PAMNs accumulate in the lesion area, l-arginine is released and metabolized in endothelial cells to produce nitric oxide (NO). The production of NO helps promote dilation and reperfusion of microvessels in the lesion area, thereby improving cerebral blood flow and reducing damage caused by stroke (Figure 7A (b)). This treatment method can not only quickly locate lesions, but also provide a new way to rebuild blood vessels in the affected area through vasodilation and thrombus aggregation relief, which helps to improve the prognosis of stroke patients[103]. These studies demonstrate the potential of inorganic nanomaterials in drug delivery, which are expected to improve therapeutic efficacy and minimize side effects through precise targeted delivery, real-time monitoring and responsive release.

3.3.2. Photodynamic Therapy

PDT, as a precise and long-term complication-reducing method for tumor treatment, relies on the synergistic interaction of light, O_2, and photosensitizers (PS) [104,105]. It generates ROS through type I or type II photochemical reaction mechanisms to eradicate cancer cells [106]. In type I reactions, the excited triplet state PS engages directly with intracellular biomolecules, initiating the formation of radical cations or anions. These radicals then interact with O_2, producing cytotoxic ROS, including superoxide anion, hydroxyl radical, and hydrogen peroxide [107]. Conversely, in type II reactions, the excited triplet state PS efficiently transfers its energy to O_2, resulting in the production of highly toxic singlet oxygen [108]. In recent decades, the evolution of nanotechnology has heralded revolutionary enhancements in PDT. Novel inorganic nanophotosensitizers have significantly enhanced the efficacy and targeting of PDT through high extinction coefficients, surface modification capabilities, nano-size advantages, EPR effects, and multifunctional integration, opening new avenues in cancer treatment. Liu and colleagues developed a therapeutic hybrid system by attaching DTPA to C60-PEG-DTPA and combining it with a gadolinium acetate solution, resulting in the preparation of Gd^{3+}-chelated C60-PEG-DTPA-Gd under specific illumination. The complex exhibited significant anti-tumor PDT effect after intravenous injection into tumor-bearing mice and the PDT effect was confirmed by MRI signal enhancement with the correlation of tumor accumulation [109]. In 2017, Gao et al. employed DNA-guided Au-Ag plasmonic nanocomponents to craft chiral nanoparticles for cancer PDT through DNA hybridization, electrical displacement reaction and cysteine enantiomer coupling, providing a new strategy for PDT therapy [110] (Figure 7B). Concurrently, Ti_3C_2 MXene was identified as a promising candidate for PDT due to its ability to generate ROS upon specific wavelength illumination. The DOX- and HA-modified Ti_3C_2 MXene nanoplatforms exhibited good

photothermal conversion and singlet oxygen generation under 808 nm laser irradiation [111]. Due to the limited effect of single treatment modality, PDT is often used in combination with chemotherapy and PTT to form an integrated treatment regimen.

3.3.3. Photothermal Therapy

PTT is a therapeutic approach that leverages photothermal agents accumulated within the tumor to convert NIR light energy into thermal energy, leading to necrosis or apoptosis of cancer cells [112,113]. Inorganic nanomaterials exhibit significant potential for application in the field of PTT by absorbing NIR light and efficiently converting it into heat through their high extinction coefficient and localized surface plasmon resonance effect [114,115]. These materials boast the distinct advantages of elevated stability and the ability to fine-tune their physicochemical properties, which can be further augmented through strategic surface modifications to enhance their biocompatibility and targeting specificity, minimizing collateral damage to healthy tissues [116].

Precious metal photothermal agents, such as gold, silver, platinum, and palladium, are capable of absorbing laser energy and converting it into thermal energy [117]. Among these, the application of gold nanomaterials in PTT has garnered attention due to the aspect ratio-dependent absorption peak of gold nanorods and their excellent photothermal conversion efficiency [118]. However, limitations such as broad size distribution and the use of toxic cetyltrimethylammonium bromide have been identified. To address these challenges, Xia et al. successfully prepared hollow gold nanocages by electrochemical methods using silver nanocubes as templates. To facilitate controlled drug release under photothermal conditions, they strategically applied the thermosensitive polymer pNIPAAm-co-AAm to the surface of the gold nanocages, effectively sealing their openings. When subjected to NIR laser irradiation, the ensuing temperature rise precipitates the disintegration of the polymer valve, thereby unveiling the openings of the gold nanocages and enabling the targeted release of the encapsulated drug payload [119]. Pd- or Pt-based PTAs remain structurally stable under laser irradiation due to their high melting points, and scientists are working to improve their absorption in the NIR band to enhance performance. Cheng et al. synthesized ultrasmall Cu, Pt, and Pd NPs, with diameters of 1.5 nm, through a dendrimer-mediated wet chemical synthesis approach. These Pt nanoparticles bound to tumor-targeting ligands showed high tumor accumulation 24 h after injection and led to significant tumor regression after photothermal treatment [120]. Additionally, Pd or Pt-based PTAs possess catalytic properties, which can be leveraged to enhance overall therapeutic efficacy [121]. Liu et al. constructed a biomimetic nanoimmune activator CuS/Z@M4T1, which is composed of ZIF-8, NIR-II photothermal agent CuS nanodots and 4T1 tumor cell membrane (Figure 7 C (a)). The homologous targeting and immune escape ability of tumor cell membrane is utilized to accumulate in tumor tissue. pH-sensitive ZIF-8 is degraded in acidic lysosomes to release CuS nanodots and Zn^{2+}. Zn^{2+} overload leads to nicotinamide adenine dinucleotide loss and reduced adenosine triphosphate level, inhibiting heat shock proteins synthesis. CuS nanodots produce photothermal effect under NIR-II laser irradiation, enhancing immunogenicity to kill cancer cells, inducing immunogenic cell death to promote dendritic cell maturation and immune cascade reaction, transforming "cold" tumors into "hot" tumors, and combining with programmed death 1 checkpoint blockade to achieve systemic immunotherapy effect, inhibiting primary tumors and delaying metastasis (Figure 7 C (b)) [122].

Graphene, owing to its unique two-dimensional structure and electronic properties, has demonstrated favorable tumor accumulation and therapeutic efficacy in PTT, despite its insolubility in water, which necessitates surface modification. The application of graphene has spurred the development of similar materials, such as transition metal dichalcogenides, transition metal oxides, and MXenes, which exhibit excellent photothermal properties and biocompatibility. For instance, Shi et al. successfully prepared molybdenum disulfide nanosheets in aqueous PEG solution using a solvothermal method. During this process, PEG chains were integrated into the nanosheet surfaces, significantly enhancing their stability and water solubility. This synthetic approach not only ensured a high yield but also allowed the nanosheets to exhibit excellent dispersion in water and maintain inherent stability under physiological conditions. Furthermore, this method allows for the modulation of nanosheet size to cater to diverse application requirements. This innovative synthesis strategy significantly facilitates the application of MoS_2 nanosheets in the biomedical field, particularly in PTT where superior dispersion and stability are required [123]. Recently, a novel graphene analogue known as MXenes has been utilized as PTAs, showing higher light absorption than reduced graphene oxide due to its higher electronic conductivity [124,125]. For example, ultrathin two-dimensional MXene tantalum carbide has a photothermal conversion efficiency that exceeds that of conventional Ti_3C_2 nanosheets and can be used as an x-ray CT contrast agent due to its high-Z elemental tantalum content [126]. This achievement not only demonstrates the high efficiency of MXene materials in PTT but also opens up new possibilities for their application in multimodal medical imaging.

3.3.4. Synergistic Therapy

Inorganic nanomaterials play an increasingly important role in disease treatment, and they significantly enhance therapeutic efficacy through precise targeted drug delivery, real-time monitoring, reactive release, and multifaceted mechanisms of action. Currently, these materials are primarily applied in combinations of PDT with PTT, PDT with chemotherapy, and PTT with chemotherapy. In particular, they show great potential in cancer therapy. Chen et al. developed chitosan hybrid nanospheres (CS-AuNR-ICG NSs) by co-loading gold nanorods (AuNR) and ICG, enabling the combined application of PTT and PDT triggered by NIR light. These nanospheres can effectively protect ICG and deliver it to the tumor site with a size of 180 nm and a wide absorption range. Under the irradiation of 808 nm laser, the high temperature and active oxygen produced by the nanospheres can effectively kill the cancer cells, which significantly improves the treatment effect [127]. The multifunctional nanoplatform based on Ti_3C_2 nanosheets (Ti_3C_2-DOX) is a novel tumor treatment system that integrates the chemotherapeutic drug doxorubicin (DOX) and the tumor-targeting agent hyaluronic acid through layer-by-layer surface modification. This nanoplatform possesses a high drug loading capacity and can achieve controlled drug release in response to pH changes in the TME. Under NIR laser irradiation, Ti_3C_2-DOX exhibits photothermal effects and triggers a photodynamic process to produce ROS, thereby exerting a synergistic killing effect on tumor cells. The development of this nanoplatform offers new possibilities for combined tumor therapy [111]. Inspired by the activation of the cGAS-STING pathway by Mn^{2+}, researchers developed a combined photothermal/immunotherapy strategy for triple-negative breast cancer (TNBC) and constructed a Mn-enriched photonic nanomedicine (MnPB-MnOx). Mn-doped prussian blue (MnPB) nanoparticles were synthesized by replacing iron with Mn^{2+}, and MnOx was bonded to the surface of MnPB by the redox reaction of polyvinylpyrrolidone and potassium permanganate to prepare MnPB-MnOx (Figure 7D(a)). Under NIR light irradiation, the nanostructure caused a double blow to tumor cells through the high temperature generated by MnPB and the ROS catalyzed by MnOx, releasing a large amount of tumor-associated antigens (TAAs) and activating the immune response. The Mn^{2+}-enhanced cGAS-STING signaling pathway promotes immune cells to secrete cytokines, mature dendritic cells and migrate to lymph nodes, activating adaptive immune responses. This increases the enrichment of natural killer cells, macrophages, and $CD8^+$ T cells at the tumor site, enhances local immunotherapy effects, and activates systemic immune responses to suppress distant tumors. Therefore, MnPB-MnOx synergistically enhances anti-tumor immunity by activating the cGAS-STING pathway and releasing TAAs, achieving enhanced local and systemic therapeutic effects (Figure 7D(b)) [128]. The combination therapy strategies utilizing inorganic nanomaterials demonstrate significant potential and broad prospects in clinical applications, particularly in cancer treatment. By employing multimodal therapeutic approaches, these strategies can effectively enhance treatment efficacy and reduce side effects.

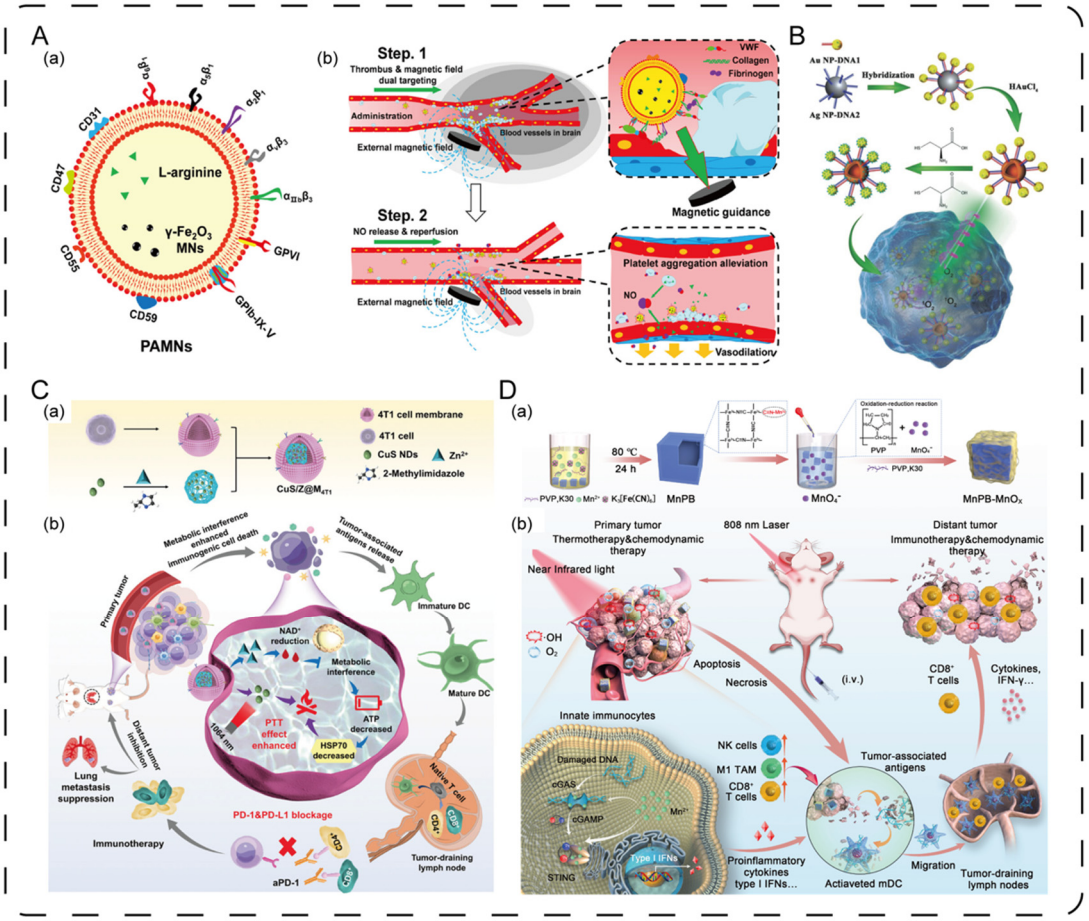

Figure 7. Application of inorganic nanomaterials in clinical treatment. (A) Schematic structure of PAMNs and in vivo targeting mechanism [103]. Copyright 2020, American Chemical Society (B) Mechanism of self-assembled shell satellite nanostructures as chiral photodynamic therapeutic agents [110]. Copyright 2017, WILEY-VCH Verlag GmbH & Co. KGaA, Weinheim. (C) Preparation method and mechanism of action of biomimetic nanoimmune activator CuS/Z@M4T$_1$ [122]. Copyright 2023, Wiley-VCH GmbH. (D) Construction of manganese-rich MnPB-MnOx nanomedicine and the mechanism of synergistic photothermal ablation and Mn^{2+}-enhanced cancer immunotherapy [128]. Copyright 2022, Elsevier Ltd.

4. Challenges and Prospects

Over the past several decades, inorganic nanomaterials have undergone remarkable advances, with our comprehension of their physicochemical characteristics and their interplay with biological systems substantially enhanced. Nonetheless, the application of inorganic nanomaterials in diseases treatment continues to be an emerging and dynamic field, given the swift progression and expansive nature of related research. The development of these materials is confronted with a myriad of challenges that substantially impede their efficacy and success in clinical settings (Figure 8).

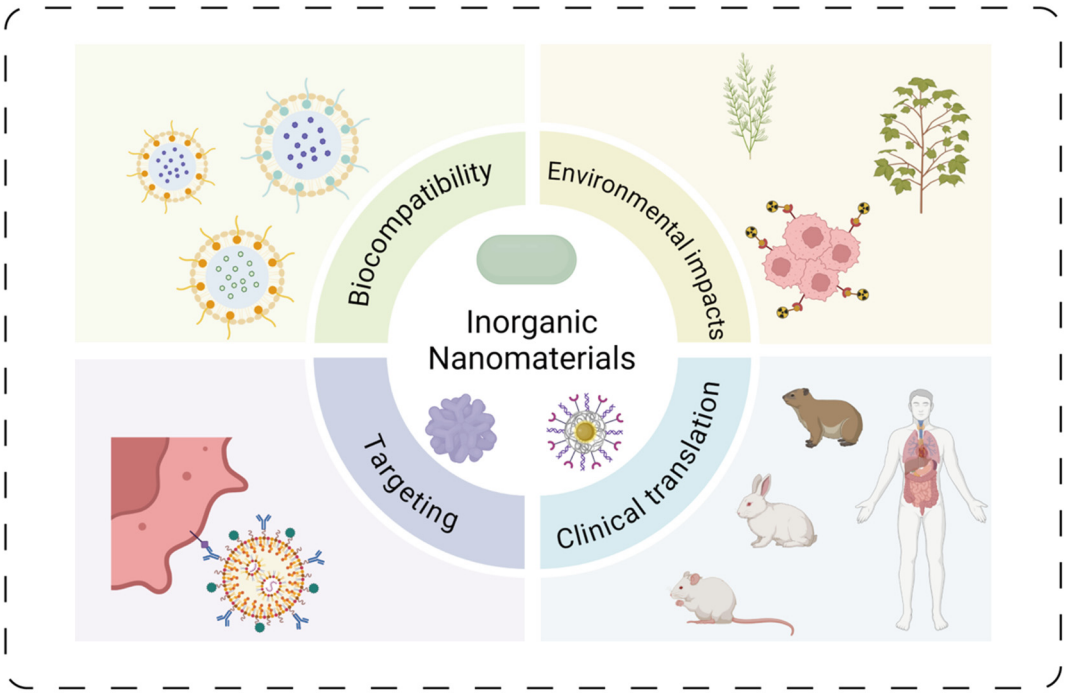

Figure 8. Challenges in the application of inorganic nanomaterials in disease treatment.

a) Biocompatibility

Inorganic nanomaterials represent a diverse array of substances, yet not all have been extensively evaluated in the human body. This raises a significant challenge in ascertaining their biocompatibility. Most of our current toxicity research is centered on conventional materials, but nanomaterials differ markedly from their bulk counterparts in terms of properties. Consequently, traditional toxicological assessments may fall short in accurately gauging or evaluating their potential toxicity. Although initial studies suggest that inorganic nanomaterials are non-toxic and capable of biodegradation, the long-term implications of their use remain unclear. Moreover, these nanomaterials may accumulate at elevated concentrations in organs such as the liver, spleen, and lungs. Therefore, it is imperative to conduct comprehensive long-term toxicity studies on inorganic nanomaterials prior to initiating clinical trials for nanomedicines.

b) Targeting

Inorganic nanomaterials for biomedical applications face challenges of targeting and drug delivery efficiency, which include achieving specific recognition of diseased cells, avoiding non-specific uptake, ensuring adequate drug loading and stability, releasing the drug at the target region on demand, penetrating vascular and cell membrane barriers, prolonging the circulation time, improving clearance, and controlling dosage accurately and taking into account individual differences in clinical applications, and these challenges need to be overcome through interdisciplinary collaboration and innovative design.

c) Clinical translation

In the development of nanomedicines, researchers face challenges in clinical translation due to the inability of animal models to fully simulate human diseases. To overcome these challenges, they must carefully select animal models that closely match human disease characteristics and use advanced imaging and bioanalytical techniques to track the distribution and effects of drugs within animals. These methods help to enhance the reliability and predictive accuracy of experimental results, laying a solid foundation for the clinical application of nanomedicines. In essence, the clinical translation of nanomedicines is an intricate endeavor that necessitates a comprehensive consideration of factors including cost, safety, formulation complexity, and environmental impact. By undertaking these meticulous evaluations and strategic refinements, the pathway for the sustainable development and clinical adoption of nanomedicines can be smoothed, ultimately offering patients with enhanced safety and efficacy in their therapeutic options.

d) Environmental impacts

Furthermore, as global consciousness regarding environmental stewardship intensifies, the ecological footprint of commercial production has garnered heightened attention. This extends beyond the potential

environmental repercussions of the nanomaterials themselves to encompass critical issues such as the management of industrial waste produced during manufacturing and energy consumption. Therefore, the development of environmentally friendly nanomedicine production and disposal technologies, alongside efforts to refine production processes to mitigate environmental impact, has emerged as a pivotal area of contemporary research.

In summary, although inorganic nanomaterials show great potential in the biomedical field, their application in the treatment of diseases still faces many challenges. With technological innovation and interdisciplinary collaboration, it is expected that these challenges can be addressed, facilitating the broad application of inorganic nanomaterials in the medical field.

Author Contributions: Conceptualization, L.L. and M.C.; methodology, L.L.; software, L.L.; validation, Y.D. and M.C.; formal analysis, L.L.; investigation, Y.D.; resources, M.C.; data curation, M.C.; writing-original draft preparation, L.L.; writing-review and editing, M.C.; visualization, Y.D.; supervision, M.C.; project administration, M.C.; All authors have read and agreed to the published version of the manuscript.

Funding: This research received no external funding.

Data Availability Statement: Not applicable.

Conflicts of Interest: The authors declare no conflict of interest.

References

1. Majumder, J.; Taratula, O.; Minko, T. Nanocarrier-based systems for targeted and site specific therapeutic delivery. *Adv. Drug Deliv. Rev.* **2019**, *144*, 57−77. DOI: 10.1016/j.addr.2019.07.010.
2. Xu, B.; Li, S.; Shi, R.; Liu, H. Multifunctional mesoporous silica nanoparticles for biomedical applications. *Signal Transduct. Target. Ther.* **2023**, *8*(1), 435. DOI: 10.1038/s41392-023-01654-7.
3. Zhang, H.; Montesdeoca, N.; Tang, D.; Liang, G.; Cui, M.; Xu, C.; Servos, L. M.; Bing, T.; Papadopoulos, Z.; Shen, M.; et al. Tumor-targeted glutathione oxidation catalysis with ruthenium nanoreactors against hypoxic osteosarcoma. *Nat. Commun.* **2024**, *15*(1), 9405. DOI: 10.1038/s41467-024-53646-y.
4. Chen, L.; Zhou, L.; Wang, C.; Han, Y.; Lu, Y.; Liu, J.; Hu, X.; Yao, T.; Lin, Y.; Liang, S.; et al. Tumor-Targeted Drug and CpG Delivery System for Phototherapy and Docetaxel-Enhanced Immunotherapy with Polarization toward M1-Type Macrophages on Triple Negative Breast Cancers. *Adv. Mater.* **2019**, *31*(52), e1904997. DOI: 10.1002/adma.201904997.
5. Zheng, K.; Setyawati, M. I.; Leong, D. T.; Xie, J. Antimicrobial Gold Nanoclusters. *ACS Nano* **2017**, *11*(7), 6904−6910. DOI: 10.1021/acsnano.7b02035.
6. Gong, X.; Jadhav, N. D.; Lonikar, V. V.; Kulkarni, A. N.; Zhang, H.; Sankapal, B. R.; Ren, J.; Xu, B. B.; Pathan, H. M.; Ma, Y.; et al. An overview of green synthesized silver nanoparticles towards bioactive antibacterial, antimicrobial and antifungal applications. *Adv. Colloid Interface Sci.* **2024**, *323*, 103053. DOI: 10.1016/j.cis.2023.103053.
7. Kesharwani, P.; Ma, R.; Sang, L.; Fatima, M.; Sheikh, A.; Abourehab, M. A. S.; Gupta, N.; Chen, Z. S.; Zhou, Y. Gold nanoparticles and gold nanorods in the landscape of cancer therapy. *Mol. Cancer* **2023**, *22*(1), 98. DOI: 10.1186/s12943-023-01798-8.
8. Amiri, M.; Salavati-Niasari, M.; Akbari, A. Magnetic nanocarriers: Evolution of spinel ferrites for medical applications. *Adv. Colloid Interface Sci.***2019**, *265*, 29−44. DOI: 10.1016/j.cis.2019.01.003.
9. Zhu, X.; Li, S. Nanomaterials in tumor immunotherapy: new strategies and challenges. *Mol. Cancer* **2023**, *22*(1), 94. DOI: 10.1186/s12943-023-01797-9.
10. Seidi, F.; Zhong, Y.; Xiao, H.; Jin, Y.; Crespy, D. Degradable polyprodrugs: design and therapeutic efficiency. *Chem. Soc. Rev.* **2022**, *51*(15), 6652−6703. DOI: 10.1039/d2cs00099g.
11. Wang, X.; Zhong, X.; Li, J.; Liu, Z.; Cheng, L. Inorganic nanomaterials with rapid clearance for biomedical applications. *Chem. Soc. Rev.* **2021**, *50*(15), 8669−8742. DOI: 10.1039/d0cs00461h.
12. Sobhanan, J.; Rival, J. V.; Anas, A.; Sidharth Shibu, E.; Takano, Y.; Biju, V. Luminescent quantum dots: Synthesis, optical properties, bioimaging and toxicity. *Adv. Drug Deliv. Rev.* **2023**, *197*, 114830. DOI: 10.1016/j.addr.2023.114830.
13. Yang, J.; Feng, J.; Yang, S.; Xu, Y.; Shen, Z. Exceedingly Small Magnetic Iron Oxide Nanoparticles for T(1)-Weighted Magnetic Resonance Imaging and Imaging-Guided Therapy of Tumors. *Small* **2023**, *19*(49), e2302856. DOI: 10.1002/smll.202302856.
14. Li, F.; Chen, L.; Zhong, S.; Chen, J.; Cao, Y.; Yu, H.; Ran, H.; Yin, Y.; Reutelingsperger, C.; Shu, S.; et al. Collagen-Targeting Self-Assembled Nanoprobes for Multimodal Molecular Imaging and Quantification of Myocardial Fibrosis in a Rat Model of Myocardial Infarction. *ACS Nano* **2024**, *18*(6), 4886−4902. DOI: 10.1021/acsnano.3c09801.
15. Xu, M.; Lin, Y.; Li, Y.; Dong, Y.; Guo, C.; Zhou, X.; Wang, L. Nanoprobe Based on Novel NIR-II Quinolinium Cyanine for Multimodal Imaging. *Small* **2024**, *20*(49), e2406879. DOI: 10.1002/smll.202406879.
16. Bi, X.; Bai, Q.; Liang, M.; Yang, D.; Li, S.; Wang, L.; Liu, J.; Yu, W. W.; Sui, N.; Zhu, Z. Silver Peroxide Nanoparticles

for Combined Antibacterial Sonodynamic and Photothermal Therapy. *Small* **2022**, *18*(2), e2104160. DOI: 10.1002/smll.202104160.

17. Zhu, X.; Wang, J.; Cai, L.; Wu, Y.; Ji, M.; Jiang, H.; Chen, J. Dissection of the antibacterial mechanism of zinc oxide nanoparticles with manipulable nanoscale morphologies. *J. Hazard Mater.* **2022**, *430*, 128436. DOI: 10.1016/j.jhazmat.2022.128436.
18. Liu, Y.; Zhao, Y.; Guo, S.; Qin, D.; Yan, J.; Cheng, H.; Zhou, J.; Ren, J.; Sun, L.; Peng, H.; et al. Copper doped carbon dots modified bacterial cellulose with enhanced antibacterial and immune regulatory functions for accelerating wound healing. *Carbohydr Polym* **2024**, *346*, 122656. DOI: 10.1016/j.carbpol.2024.122656.
19. Salah, M.; Akasaka, H.; Shimizu, Y.; Morita, K.; Nishimura, Y.; Kubota, H.; Kawaguchi, H.; Sogawa, T.; Mukumoto, N.; Ogino, C.; et al. Reactive oxygen species-inducing titanium peroxide nanoparticles as promising radiosensitizers for eliminating pancreatic cancer stem cells. *J. Exp. Clin. Cancer Res.* **2022**, *41*(1), 146. DOI: 10.1186/s13046-022-02358-6.
20. Vallet-Regí, M.; Schüth, F.; Lozano, D.; Colilla, M.; Manzano, M. Engineering mesoporous silica nanoparticles for drug delivery: where are we after two decades? *Chem. Soc. Rev.* **2022**, *51*(13), 5365−5451. DOI: 10.1039/d1cs00659b.
21. Khan, S.; Falahati, M.; Cho, W. C.; Vahdani, Y.; Siddique, R.; Sharifi, M.; Jaragh-Alhadad, L. A.; Haghighat, S.; Zhang, X.; Ten Hagen, T. L. M.; et al. Core-shell inorganic NP@MOF nanostructures for targeted drug delivery and multimodal imaging-guided combination tumor treatment. *Adv. Colloid Interface Sci.* **2023**, *321*, 103007. DOI: 10.1016/j.cis.2023.103007.
22. Arvizo, R. R.; Bhattacharyya, S.; Kudgus, R. A.; Giri, K.; Bhattacharya, R.; Mukherjee, P. Intrinsic therapeutic applications of noble metal nanoparticles: past, present and future. *Chem. Soc. Rev.* **2012**, *41*(7), 2943−2970. DOI: 10.1039/c2cs15355f.
23. Hao, R.; Xing, R.; Xu, Z.; Hou, Y.; Gao, S.; Sun, S. Synthesis, functionalization, and biomedical applications of multifunctional magnetic nanoparticles. *Adv. Mater.* **2010**, *22*(25), 2729−2742. DOI: 10.1002/adma.201000260.
24. Fan, H.; Yan, G.; Zhao, Z.; Hu, X.; Zhang, W.; Liu, H.; Fu, X.; Fu, T.; Zhang, X.-B.; Tan, W. A Smart Photosensitizer-Manganese Dioxide Nanosystem for Enhanced Photodynamic Therapy by Reducing Glutathione Levels in Cancer Cells. *Angew. Chem. Int. Ed. Engl.* **2016**, *55*(18), 5477−5482. DOI: 10.1002/anie.201510748.
25. Zhu, W.; Dong, Z.; Fu, T.; Liu, J.; Chen, Q.; Li, Y.; Zhu, R.; Xu, L.; Liu, Z. Modulation of Hypoxia in Solid Tumor Microenvironment with MnO2 Nanoparticles to Enhance Photodynamic Therapy. *Adv. Funct. Mater.* **2016**, *26*(30), 5490-5498. DOI: 10.1002/adfm.201600676.
26. Chen, Y.; Ye, D.; Wu, M.; Chen, H.; Zhang, L.; Shi, J.; Wang, L. Break-up of two-dimensional MnO2 nanosheets promotes ultrasensitive pH-triggered theranostics of cancer. *Adv. Mater.* **2014**, *26*(41), 7019 − 7026. DOI: 10.1002/adma.201402572.
27. Chen, Q.; Feng, L.; Liu, J.; Zhu, W.; Dong, Z.; Wu, Y.; Liu, Z. Intelligent Albumin-MnO2 Nanoparticles as pH-/H2 O2 -Responsive Dissociable Nanocarriers to Modulate Tumor Hypoxia for Effective Combination Therapy. *Adv. Mater.* **2016**, *28*(33), 7129−7136. DOI: 10.1002/adma.201601902.
28. Dong, Z.; Feng, L.; Zhu, W.; Sun, X.; Gao, M.; Zhao, H.; Chao, Y.; Liu, Z. CaCO(3) nanoparticles as an ultra-sensitive tumor-pH-responsive nanoplatform enabling real-time drug release monitoring and cancer combination therapy. *Biomater.* **2016**, *110*, 60−70. DOI: 10.1016/j.biomaterials.2016.09.025.
29. Xu, L.; Tong, G.; Song, Q.; Zhu, C.; Zhang, H.; Shi, J.; Zhang, Z. Enhanced Intracellular Ca(2+) Nanogenerator for Tumor-Specific Synergistic Therapy via Disruption of Mitochondrial Ca(2+) Homeostasis and Photothermal Therapy. *ACS Nano* **2018**, *12*(7), 6806−6818. DOI: 10.1021/acsnano.8b02034.
30. Hao, J.; Song, G.; Liu, T.; Yi, X.; Yang, K.; Cheng, L.; Liu, Z. In Vivo Long-Term Biodistribution, Excretion, and Toxicology of PEGylated Transition-Metal Dichalcogenides MS2 (M = Mo, W, Ti) Nanosheets. *Adv. Sci. (Weinh.)* **2017**, *4*(1), 1600160. DOI: 10.1002/advs.201600160.
31. Zhou, M.; Li, J.; Liang, S.; Sood, A. K.; Liang, D.; Li, C. CuS Nanodots with Ultrahigh Efficient Renal Clearance for Positron Emission Tomography Imaging and Image-Guided Photothermal Therapy. *ACS Nano* **2015**, *9*(7), 7085−7096. DOI: 10.1021/acsnano.5b02635.
32. Wang, L.; Xu, D.; Jiang, L.; Gao, J.; Tang, Z.; Xu, Y.; Chen, X.; Zhang, H. Transition Metal Dichalcogenides for Sensing and Oncotherapy: Status, Challenges, and Perspective. *Adv. Funct. Mater.* **2020**, *31*(5). DOI: 10.1002/adfm.202004408.
33. Yang, S. M.; Shim, J. H.; Cho, H. U.; Jang, T. M.; Ko, G. J.; Shim, J.; Kim, T. H.; Zhu, J.; Park, S.; Kim, Y. S.; et al. Hetero-Integration of Silicon Nanomembranes with 2D Materials for Bioresorbable, Wireless Neurochemical System. *Adv. Mater.* **2022**, *34*(14), e2108203. DOI: 10.1002/adma.202108203.
34. Zhu, S.; Meng, Q.; Wang, L.; Zhang, J.; Song, Y.; Jin, H.; Zhang, K.; Sun, H.; Wang, H.; Yang, B. Highly photoluminescent carbon dots for multicolor patterning, sensors, and bioimaging. *Angew. Chem. Int. Ed. Engl.* **2013**,

52(14), 3953−3957. DOI: 10.1002/anie.201300519.

35. Feng, T.; Ai, X.; Ong, H.; Zhao, Y. Dual-Responsive Carbon Dots for Tumor Extracellular Microenvironment Triggered Targeting and Enhanced Anticancer Drug Delivery. *ACS Appl. Mater. Interfaces* **2016**, *8*(29), 18732−18740. DOI: 10.1021/acsami.6b06695.
36. Feng, T.; Ai, X.; An, G.; Yang, P.; Zhao, Y. Charge-Convertible Carbon Dots for Imaging-Guided Drug Delivery with Enhanced in Vivo Cancer Therapeutic Efficiency. *ACS Nano* **2016**, *10*(4), 4410−4420. DOI: 10.1021/acsnano.6b00043.
37. Huang, P.; Lin, J.; Wang, X.; Wang, Z.; Zhang, C.; He, M.; Wang, K.; Chen, F.; Li, Z.; Shen, G.; et al. Light-triggered theranostics based on photosensitizer-conjugated carbon dots for simultaneous enhanced-fluorescence imaging and photodynamic therapy. *Adv. Mater.* **2012**, *24*(37), 5104−5110. DOI: 10.1002/adma.201200650.
38. Huang, X.; Zhang, F.; Zhu, L.; Choi, K. Y.; Guo, N.; Guo, J.; Tackett, K.; Anilkumar, P.; Liu, G.; Quan, Q.; et al. Effect of injection routes on the biodistribution, clearance, and tumor uptake of carbon dots. *ACS Nano* **2013**, *7*(7), 5684−5693. DOI: 10.1021/nn401911k.
39. Licciardello, N.; Hunoldt, S.; Bergmann, R.; Singh, G.; Mamat, C.; Faramus, A.; Ddungu, J. L. Z.; Silvestrini, S.; Maggini, M.; De Cola, L.; et al. Biodistribution studies of ultrasmall silicon nanoparticles and carbon dots in experimental rats and tumor mice. *Nanoscale* **2018**, *10*(21), 9880−9891. DOI: 10.1039/c8nr01063c.
40. Wang, S.; Li, C.; Qian, M.; Jiang, H.; Shi, W.; Chen, J.; Lächelt, U.; Wagner, E.; Lu, W.; Wang, Y.; et al. Augmented glioma-targeted theranostics using multifunctional polymer-coated carbon nanodots. *Biomater.* **2017**, *141*, 29−39. DOI: 10.1016/j.biomaterials.2017.05.040.
41. Iannazzo, D.; Ziccarelli, I.; Pistone, A. Graphene quantum dots: multifunctional nanoplatforms for anticancer therapy. *J. Mater. Chem. B* **2017**, *5*(32), 6471−6489. DOI: 10.1039/c7tb00747g.
42. Lee, C.; Kwon, W.; Beack, S.; Lee, D.; Park, Y.; Kim, H.; Hahn, S. K.; Rhee, S.-W.; Kim, C. Biodegradable Nitrogen-Doped Carbon Nanodots for Non-Invasive Photoacoustic Imaging and Photothermal Therapy. *Theranostics* **2016**, *6*(12), 2196−2208..
43. Chong, Y.; Ma, Y.; Shen, H.; Tu, X.; Zhou, X.; Xu, J.; Dai, J.; Fan, S.; Zhang, Z. The in vitro and in vivo toxicity of graphene quantum dots. *Biomater.* **2014**, *35*(19), 5041−5048. DOI: 10.1016/j.biomaterials.2014.03.021.
44. Yan, H.; Wang, Q.; Wang, J.; Shang, W.; Xiong, Z.; Zhao, L.; Sun, X.; Tian, J.; Kang, F.; Yun, S.-H. Planted Graphene Quantum Dots for Targeted, Enhanced Tumor Imaging and Long-Term Visualization of Local Pharmacokinetics. *Adv. Mater.* **2023**, *35*(15), e2210809. DOI: 10.1002/adma.202210809.
45. Yu, W. W.; Chang, E.; Drezek, R.; Colvin, V. L. Water-soluble quantum dots for biomedical applications. *Biochem Biophys. Res. Commun.* **2006**, *348*(3), 781−786..
46. Zhang, W.; Chen, G.; Wang, J.; Ye, B.-C.; Zhong, X. Design and synthesis of highly luminescent near-infrared-emitting water-soluble CdTe/CdSe/ZnS core/shell/shell quantum dots. *Inorg. Chem.* **2009**, *48*(20), 9723 − 9731. DOI: 10.1021/ic9010949.
47. Liu, W.; Choi, H. S.; Zimmer, J. P.; Tanaka, E.; Frangioni, J. V.; Bawendi, M. Compact cysteine-coated CdSe(ZnCdS) quantum dots for in vivo applications. *J. Am. Chem. Soc.* **2007**, *129*(47), 14530−14531..
48. Haque, M.; Kalita, M.; Chamlagai, D.; Lyndem, S.; Koley, S.; Kumari, P.; Aguan, K.; Singha Roy, A. Human serum albumin directed formation of cadmium telluride quantum dots: Applications in biosensing, anti-bacterial activities and cell cytotoxicity measurements. *Int. J. Biol. Macromol.* **2024**, *268*(Pt 1), 131862. DOI: 10.1016/j.ijbiomac.2024.131862.
49. Ma, N.; Marshall, A. F.; Gambhir, S. S.; Rao, J. Facile synthesis, silanization, and biodistribution of biocompatible quantum dots. *Small* **2010**, *6*(14), 1520−1528. DOI: 10.1002/smll.200902409.
50. Su, Y.; Ji, X.; He, Y. Water-Dispersible Fluorescent Silicon Nanoparticles and their Optical Applications. *Adv. Mater.* **2016**, *28*(47), 10567−10574. DOI: 10.1002/adma.201601173.
51. Tang, J.; Chu, B.; Wang, J.; Song, B.; Su, Y.; Wang, H.; He, Y. Multifunctional nanoagents for ultrasensitive imaging and photoactive killing of Gram-negative and Gram-positive bacteria. *Nat. Commun.* **2019**, *10*(1), 4057. DOI: 10.1038/s41467-019-12088-7.
52. Benezra, M.; Penate-Medina, O.; Zanzonico, P. B.; Schaer, D.; Ow, H.; Burns, A.; DeStanchina, E.; Longo, V.; Herz, E.; Iyer, S.; et al. Multimodal silica nanoparticles are effective cancer-targeted probes in a model of human melanoma. *J. Clin. Invest.* **2011**, *121*(7), 2768−2780. DOI: 10.1172/JCI45600.
53. Jokerst, J. V.; Gambhir, S. S. Molecular imaging with theranostic nanoparticles. *Acc. Chem. Res.* **2011**, *44*(10), 1050−1060. DOI: 10.1021/ar200106e.
54. Erogbogbo, F.; Yong, K.-T.; Hu, R.; Law, W.-C.; Ding, H.; Chang, C.-W.; Prasad, P. N.; Swihart, M. T. Biocompatible magnetofluorescent probes: luminescent silicon quantum dots coupled with superparamagnetic iron(III) oxide. *ACS Nano*

2010, *4*(9), 5131−5138. DOI: 10.1021/nn101016f.

55. Hanada, S.; Fujioka, K.; Futamura, Y.; Manabe, N.; Hoshino, A.; Yamamoto, K. Evaluation of anti-inflammatory drug-conjugated silicon quantum dots: their cytotoxicity and biological effect. *Int. J. Mol. Sci.* **2013**, *14*(1), 1323−1334. DOI: 10.3390/ijms14011323.
56. Chen, G.; Teng, Z.; Su, X.; Liu, Y.; Lu, G. Unique Biological Degradation Behavior of Stöber Mesoporous Silica Nanoparticles from Their Interiors to Their Exteriors. *J. Biomed Nanotechnol.* **2015**, *11*(4), 722−729..
57. Yamada, H.; Urata, C.; Aoyama, Y.; Osada, S.; Yamauchi, Y.; Kuroda, K. Preparation of Colloidal Mesoporous Silica Nanoparticles with Different Diameters and Their Unique Degradation Behavior in Static Aqueous Systems. *Chem. Mater.* **2012**, *24*(8), 1462−1471. DOI: 10.1021/cm3001688.
58. He, Q.; Shi, J.; Zhu, M.; Chen, Y.; Chen, F. The three-stage in vitro degradation behavior of mesoporous silica in simulated body fluid. *Microporous Mesoporous Mater.* **2010**, *131*(1−3), 314−320. DOI: 10.1016/j.micromeso.2010.01.009.
59. Toy, R.; Peiris, P. M.; Ghaghada, K. B.; Karathanasis, E. Shaping cancer nanomedicine: the effect of particle shape on the in vivo journey of nanoparticles. *Nanomed. (Lond)* **2014**, *9*(1), 121−134. DOI: 10.2217/nnm.13.191.
60. Truong, N. P.; Whittaker, M. R.; Mak, C. W.; Davis, T. P. The importance of nanoparticle shape in cancer drug delivery. *Expert Opin. Drug. Deliv.* **2015**, *12*(1), 129−142. DOI: 10.1517/17425247.2014.950564.
61. Huang, X.; Li, L.; Liu, T.; Hao, N.; Liu, H.; Chen, D.; Tang, F. The shape effect of mesoporous silica nanoparticles on biodistribution, clearance, and biocompatibility in vivo. *ACS Nano* **2011**, *5*(7), 5390−5399. DOI: 10.1021/nn200365a.
62. He, Q.; Zhang, Z.; Gao, F.; Li, Y.; Shi, J. In vivo biodistribution and urinary excretion of mesoporous silica nanoparticles: effects of particle size and PEGylation. *Small* **2011**, *7*(2), 271−280. DOI: 10.1002/smll.201001459.
63. Cauda, V.; Argyo, C.; Bein, T. Impact of different PEGylation patterns on the long-term bio-stability of colloidal mesoporous silica nanoparticles. *J. Mater. Chem.* **2010**, *20*(39). DOI: 10.1039/c0jm01390k.
64. He, X.; Nie, H.; Wang, K.; Tan, W.; Wu, X.; Zhang, P. In vivo study of biodistribution and urinary excretion of surface-modified silica nanoparticles. *Anal. Chem.* **2008**, *80*(24), 9597−9603. DOI: 10.1021/ac801882g.
65. Vivero-Escoto, J. L.; Taylor-Pashow, K. M.; Huxford, R. C.; Della Rocca, J.; Okoruwa, C.; An, H.; Lin, W.; Lin, W. Multifunctional mesoporous silica nanospheres with cleavable Gd(III) chelates as MRI contrast agents: synthesis, characterization, target-specificity, and renal clearance. *Small* **2011**, *7*(24), 3519−3528. DOI: 10.1002/smll.201100521.
66. Souris, J. S.; Lee, C.-H.; Cheng, S.-H.; Chen, C.-T.; Yang, C.-S.; Ho, J.-a. A.; Mou, C.-Y.; Lo, L.-W. Surface charge-mediated rapid hepatobiliary excretion of mesoporous silica nanoparticles. *Biomater.* **2010**, *31*(21), 5564−5574. DOI: 10.1016/j.biomaterials.2010.03.048.
67. Wang, C.; Yan, C.; An, L.; Zhao, H.; Song, S.; Yang, S. Fe3O4 assembly for tumor accurate diagnosis by endogenous GSH responsive T2/T1 magnetic relaxation conversion. *J. Mater. Chem. B* **2021**, *9*(37), 7734 − 7740. DOI: 10.1039/d1tb01018b.
68. Guan, G.; Zhang, C.; Liu, H.; Wang, Y.; Dong, Z.; Lu, C.; Nan, B.; Yue, R.; Yin, X.; Zhang, X. B.; et al. Ternary Alloy PtWMn as a Mn Nanoreservoir for High-Field MRI Monitoring and Highly Selective Ferroptosis Therapy. *Angew. Chem. Int. Ed. Engl.* **2022**, *61*(31), e202117229. DOI: 10.1002/anie.202117229.
69. Liu, Y.; Teng, L.; Yin, B.; Meng, H.; Yin, X.; Huan, S.; Song, G.; Zhang, X.-B. Chemical Design of Activatable Photoacoustic Probes for Precise Biomedical Applications. *Chem. Rev.* **2022**, *122*(6), 6850 − 6918. DOI: 10.1021/acs.chemrev.1c00875.
70. Zeng, J.; Cheng, M.; Wang, Y.; Wen, L.; Chen, L.; Li, Z.; Wu, Y.; Gao, M.; Chai, Z. pH-Responsive Fe(III)-Gallic Acid Nanoparticles for In Vivo Photoacoustic-Imaging-Guided Photothermal Therapy. *Adv. Healthc. Mater.* **2016**, *5*(7), 772−780. DOI: 10.1002/adhm.201500898.
71. Wang, S.; Zhang, L.; Zhao, J.; He, M.; Huang, Y.; Zhao, S. A tumor microenvironment-induced absorption red-shifted polymer nanoparticle for simultaneously activated photoacoustic imaging and photothermal therapy. *Sci. Adv.* **2021**, *7*(12). DOI: 10.1126/sciadv.abe3588.
72. Zhang, W.; Wang, J.; Su, L.; Chen, H.; Zhang, L.; Lin, L.; Chen, X.; Song, J.; Yang, H. Activatable nanoscale metal-organic framework for ratiometric photoacoustic imaging of hydrogen sulfide and orthotopic colorectal cancer in vivo. *Sci. China Chem.* **2020**, *63*(9), 1315−1322. DOI: 10.1007/s11426-020-9775-y.
73. Zhao, J.; Jin, G.; Weng, G.; Li, J.; Zhu, J.; Zhao, J. Recent advances in activatable fluorescence imaging probes for tumor imaging. *Drug Discov. Today* **2017**, *22*(9), 1367−1374. DOI: 10.1016/j.drudis.2017.04.006.
74. Yang, W.; Yang, S.; Jiang, L.; Zhou, Y.; Yang, C.; Deng, C. Tumor microenvironment triggered biodegradation of inorganic nanoparticles for enhanced tumor theranostics. *RSC Adv.* **2020**, *10*(45), 26742 − 26751. DOI: 10.1039/d0ra04651e.

75. Liu, F.; Li, X.-L.; Zhou, H. Biodegradable MnO2 nanosheet based DNAzyme-recycling amplification towards: Sensitive detection of intracellular MicroRNAs. *Talanta* **2020**, *206*, 120199. DOI: 10.1016/j.talanta.2019.120199.
76. Wei, M.; Bai, J.; Shen, X.; Lou, K.; Gao, Y.; Lv, R.; Wang, P.; Liu, X.; Zhang, G. Glutathione-Exhausting Nanoprobes for NIR-II Fluorescence Imaging-Guided Surgery and Boosting Radiation Therapy Efficacy via Ferroptosis in Breast Cancer. *ACS Nano* **2023**, *17*(12), 11345−11361. DOI: 10.1021/acsnano.3c00350.
77. Lu, J.; Li, Z.; Lu, M.; Fan, N.; Zhang, W.; Li, P.; Tang, Y.; Yin, X.; Zhang, W.; Wang, H.; et al. Assessing Early Atherosclerosis by Detecting and Imaging of Hypochlorous Acid and Phosphorylation Using Fluorescence Nanoprobe. *Adv. Mater.* **2023**, *35*(52), e2307008. DOI: 10.1002/adma.202307008.
78. Sabuncu, S.; Yildirim, A. Gas-stabilizing nanoparticles for ultrasound imaging and therapy of cancer. *Nano Converg.* **2021**, *8*(1), 39. DOI: 10.1186/s40580-021-00287-2.
79. Feng, Q.; Zhang, W.; Yang, X.; Li, Y.; Hao, Y.; Zhang, H.; Hou, L.; Zhang, Z. pH/Ultrasound Dual-Responsive Gas Generator for Ultrasound Imaging-Guided Therapeutic Inertial Cavitation and Sonodynamic Therapy. *Adv. Healthc. Mater.* **2018**, *7*(5), 1700957. DOI: 10.1002/adhm.201700957.
80. Wu, J.; Williams, G. R.; Niu, S.; Gao, F.; Tang, R.; Zhu, L.-M. A Multifunctional Biodegradable Nanocomposite for Cancer Theranostics. *Adv. Sci. (Weinh.)* **2019**, *6*(14), 1802001. DOI: 10.1002/advs.201802001.
81. Meng, X.; Yi, Y.; Meng, Y.; Lv, G.; Jiang, X.; Wu, Y.; Yang, W.; Yao, Y.; Xu, H.; Bu, W. Self-Enhanced Acoustic Impedance Difference Strategy for Detecting the Acidic Tumor Microenvironment. *ACS Nano* **2022**, *16*(3), 4217−4227. DOI: 10.1021/acsnano.1c10173.
82. Cohen, M. L. Changing patterns of infectious disease. *Nature* **2000**, *406*(6797), 762−767.
83. Huo, M.; Wang, L.; Zhang, H.; Zhang, L.; Chen, Y.; Shi, J. Construction of Single-Iron-Atom Nanocatalysts for Highly Efficient Catalytic Antibiotics. *Small* **2019**, *15*(31), e1901834. DOI: 10.1002/smll.201901834.
84. Lu, M.-M.; Ge, Y.; Qiu, J.; Shao, D.; Zhang, Y.; Bai, J.; Zheng, X.; Chang, Z.-M.; Wang, Z.; Dong, W.-F.; et al. Redox/pH dual-controlled release of chlorhexidine and silver ions from biodegradable mesoporous silica nanoparticles against oral biofilms. *Int. J. Nanomed.***2018**, *13*, 7697−7709. DOI: 10.2147/IJN.S181168.
85. Gao, L.; Wang, Y.; Li, Y.; Xu, M.; Sun, G.; Zou, T.; Wang, F.; Xu, S.; Da, J.; Wang, L. Biomimetic biodegradable Ag@Au nanoparticle-embedded ureteral stent with a constantly renewable contact-killing antimicrobial surface and antibiofilm and extraction-free properties. *Acta Biomater.* **2020**, *114*, 117−132. DOI: 10.1016/j.actbio.2020.07.025.
86. Zhang, W.; Yang, C.; Lei, Z.; Guan, G.; He, S.-A.; Zhang, Z.; Zou, R.; Shen, H.; Hu, J. New Strategy for Specific Eradication of Implant-Related Infections Based on Special and Selective Degradability of Rhenium Trioxide Nanocubes. *ACS Appl. Mater. Interfaces* **2019**, *11*(29), 25691−25701. DOI: 10.1021/acsami.9b07359.
87. Rabe, K. F.; Watz, H. Chronic obstructive pulmonary disease. *Lancet* **2017**, *389*(10082), 1931 − 1940. DOI: 10.1016/S0140-6736(17)31222-9.
88. Ti, H.; Zhou, Y.; Liang, X.; Li, R.; Ding, K.; Zhao, X. Targeted Treatments for Chronic Obstructive Pulmonary Disease (COPD) Using Low-Molecular-Weight Drugs (LMWDs). *J. Med. Chem.* **2019**, *62* (13), 5944 − 5978. DOI: 10.1021/acs.jmedchem.8b01520.
89. Li, Z.; Luo, G.; Hu, W.-P.; Hua, J.-L.; Geng, S.; Chu, P. K.; Zhang, J.; Wang, H.; Yu, X.-F. Mediated Drug Release from Nanovehicles by Black Phosphorus Quantum Dots for Efficient Therapy of Chronic Obstructive Pulmonary Disease. *Angew. Chem. Int. Ed. Engl.* **2020**, *59*(46), 20568−20576. DOI: 10.1002/anie.202008379.
90. Wang, X.; Zhong, X.; Lei, H.; Geng, Y.; Zhao, Q.; Gong, F.; Yang, Z.; Dong, Z.; Liu, Z.; Cheng, L. Hollow Cu2Se Nanozymes for Tumor Photothermal-Catalytic Therapy. *Chem. of Mater.* **2019**, *31*(16), 6174 − 6186. DOI: 10.1021/acs.chemmater.9b01958.
91. Xi, J.; Wei, G.; Wu, Q.; Xu, Z.; Liu, Y.; Han, J.; Fan, L.; Gao, L. Light-enhanced sponge-like carbon nanozyme used for synergetic antibacterial therapy. *Biomater. Sci.* **2019**, *7*(10), 4131−4141. DOI: 10.1039/c9bm00705a.
92. Xu, B.; Wang, H.; Wang, W.; Gao, L.; Li, S.; Pan, X.; Wang, H.; Yang, H.; Meng, X.; Wu, Q.; et al. A Single-Atom Nanozyme for Wound Disinfection Applications. *Angew. Chem. Int. Ed. Engl.* **2019**, *58*(15), 4911 − 4916. DOI: 10.1002/anie.201813994.
93. Yin, W.; Yu, J.; Lv, F.; Yan, L.; Zheng, L. R.; Gu, Z.; Zhao, Y. Functionalized Nano-MoS2 with Peroxidase Catalytic and Near-Infrared Photothermal Activities for Safe and Synergetic Wound Antibacterial Applications. *ACS Nano* **2016**, *10*(12), 11000−11011. DOI: 10.1021/acsnano.6b05810.
94. Liu, Y.; Guo, Z.; Li, F.; Xiao, Y.; Zhang, Y.; Bu, T.; Jia, P.; Zhe, T.; Wang, L. Multifunctional Magnetic Copper Ferrite Nanoparticles as Fenton-like Reaction and Near-Infrared Photothermal Agents for Synergetic Antibacterial Therapy. *ACS Appl. Mater. Interfaces* **2019**, *11*(35), 31649−31660. DOI: 10.1021/acsami.9b10096.
95. Wang, X.; Fan, L.; Cheng, L.; Sun, Y.; Wang, X.; Zhong, X.; Shi, Q.; Gong, F.; Yang, Y.; Ma, Y.; et al. Biodegradable

Nickel Disulfide Nanozymes with GSH-Depleting Function for High-Efficiency Photothermal-Catalytic Antibacterial Therapy. *iScience* **2020**, *23*(7), 101281. DOI: 10.1016/j.isci.2020.101281.

96. Zhang, Z.; Wang, X.; Liu, J.; Yang, H.; Tang, H.; Li, J.; Luan, S.; Yin, J.; Wang, L.; Shi, H. Structural Element of Vitamin U-Mimicking Antibacterial Polypeptide with Ultrahigh Selectivity for Effectively Treating MRSA Infections. *Angew. Chem. Int. Ed. Engl.* **2024**, *63*(7), e202318011. DOI: 10.1002/anie.202318011.
97. Lee, J. E.; Lee, N.; Kim, T.; Kim, J.; Hyeon, T. Multifunctional mesoporous silica nanocomposite nanoparticles for theranostic applications. *Acc. Chem. Res.* **2011**, *44*(10), 893−902. DOI: 10.1021/ar2000259.
98. Li, Z.; Barnes, J. C.; Bosoy, A.; Stoddart, J. F.; Zink, J. I. Mesoporous silica nanoparticles in biomedical applications. *Chem. Soc. Rev.* **2012**, *41*(7), 2590−2605. DOI: 10.1039/c1cs15246g.
99. Yang, P.; Quan, Z.; Hou, Z.; Li, C.; Kang, X.; Cheng, Z.; Lin, J. A magnetic, luminescent and mesoporous core-shell structured composite material as drug carrier. *Biomaterials* **2009**, *30*(27), 4786 − 4795. DOI: 10.1016/j.biomaterials.2009.05.038.
100. Arias, L. S.; Pessan, J. P.; Vieira, A. P. M.; Lima, T. M. T. d.; Delbem, A. C. B.; Monteiro, D. R. Iron Oxide Nanoparticles for Biomedical Applications: A Perspective on Synthesis, Drugs, Antimicrobial Activity, and Toxicity. *Antibiot. (Basel)* **2018**, *7*(2). DOI: 10.3390/antibiotics7020046.
101. Bobo, D.; Robinson, K. J.; Islam, J.; Thurecht, K. J.; Corrie, S. R. Nanoparticle-Based Medicines: A Review of FDA-Approved Materials and Clinical Trials to Date. *Pharm. Res.* **2016**, *33*(10), 2373−2387. DOI: 10.1007/s11095-016-1958-5.
102. Zhang, Y.; Fu, X.; Jia, J.; Wikerholmen, T.; Xi, K.; Kong, Y.; Wang, J.; Chen, H.; Ma, Y.; Li, Z.; et al. Glioblastoma Therapy Using Codelivery of Cisplatin and Glutathione Peroxidase Targeting siRNA from Iron Oxide Nanoparticles. *ACS Appl. Mater. Interfaces* **2020**, *12*(39), 43408−43421. DOI: 10.1021/acsami.0c12042.
103. Li, M.; Li, J.; Chen, J.; Liu, Y.; Cheng, X.; Yang, F.; Gu, N. Platelet Membrane Biomimetic Magnetic Nanocarriers for Targeted Delivery and in Situ Generation of Nitric Oxide in Early Ischemic Stroke. *ACS Nano* **2020**, *14*(2), 2024−2035. DOI: 10.1021/acsnano.9b08587.
104. Voon, S. H.; Kiew, L. V.; Lee, H. B.; Lim, S. H.; Noordin, M. I.; Kamkaew, A.; Burgess, K.; Chung, L. Y. In vivo studies of nanostructure-based photosensitizers for photodynamic cancer therapy. *Small* **2014**, *10*(24), 4993 − 5013. DOI: 10.1002/smll.201401416.
105. Felsher, D. W. Cancer revoked: oncogenes as therapeutic targets. *Nat. Rev. Cancer.* **2003**, *3*(5), 375−380.
106. Agostinis, P.; Berg, K.; Cengel, K. A.; Foster, T. H.; Girotti, A. W.; Gollnick, S. O.; Hahn, S. M.; Hamblin, M. R.; Juzeniene, A.; Kessel, D.; et al. Photodynamic therapy of cancer: an update. *CA Cancer J. Clin.* **2011**, *61*(4), 250−281. DOI: 10.3322/caac.20114.
107. Plaetzer, K.; Krammer, B.; Berlanda, J.; Berr, F.; Kiesslich, T. Photophysics and photochemistry of photodynamic therapy: fundamental aspects. *Lasers Med. Sci.* **2009**, *24*(2), 259−268. DOI: 10.1007/s10103-008-0539-1.
108. Zhao, J.; Wu, W.; Sun, J.; Guo, S. Triplet photosensitizers: from molecular design to applications. *Chem. Soc. Rev.* **2013**, *42*(12), 5323−5351. DOI: 10.1039/c3cs35531d.
109. Liu, J.; Ohta, S.-I.; Sonoda, A.; Yamada, M.; Yamamoto, M.; Nitta, N.; Murata, K.; Tabata, Y. Preparation of PEG-conjugated fullerene containing Gd3+ ions for photodynamic therapy. *J. Control Release* **2007**, *117*(1), 104−110.
110. Gao, F.; Sun, M.; Ma, W.; Wu, X.; Liu, L.; Kuang, H.; Xu, C. A Singlet Oxygen Generating Agent by Chirality-dependent Plasmonic Shell-Satellite Nanoassembly. *Adv. Mater.* **2017**, *29*(18), 1606864. DOI: 10.1002/adma.201606864.
111. Liu, G.; Zou, J.; Tang, Q.; Yang, X.; Zhang, Y.; Zhang, Q.; Huang, W.; Chen, P.; Shao, J.; Dong, X. Surface Modified Ti3C2 MXene Nanosheets for Tumor Targeting Photothermal/Photodynamic/Chemo Synergistic Therapy. *ACS Appl. Mater. Interfaces* **2017**, *9*(46), 40077−40086. DOI: 10.1021/acsami.7b13421.
112. Yang, K.; Zhang, S.; Zhang, G.; Sun, X.; Lee, S.-T.; Liu, Z. Graphene in mice: ultrahigh in vivo tumor uptake and efficient photothermal therapy. *Nano Lett.* **2010**, *10*(9), 3318−3323. DOI: 10.1021/nl100996u.
113. Melamed, J. R.; Edelstein, R. S.; Day, E. S. Elucidating the fundamental mechanisms of cell death triggered by photothermal therapy. *ACS Nano* **2015**, *9*(1). DOI: 10.1021/acsnano.5b00021.
114. Fernandes, N.; Rodrigues, C. F.; Moreira, A. F.; Correia, I. J. Overview of the application of inorganic nanomaterials in cancer photothermal therapy. *Biomater. Sci.* **2020**, *8* (11), 2990−3020. DOI: 10.1039/d0bm00222d.
115. Gellini, C.; Feis, A. Optothermal properties of plasmonic inorganic nanoparticles for photoacoustic applications. *Photoacoust.* **2021**, *23*, 100281. DOI: 10.1016/j.pacs.2021.100281.
116. Wang, J.; Wu, X.; Shen, P.; Wang, J.; Shen, Y.; Shen, Y.; Webster, T. J.; Deng, J. Applications of Inorganic Nanomaterials in Photothermal Therapy Based on Combinational Cancer Treatment. *Int. J. Nanomed.***2020**, *15*, 1903−1914. DOI: 10.2147/IJN.S239751.

117. Gai, S.; Yang, G.; Yang, P.; He, F.; Lin, J.; Jin, D.; Xing, B. Recent advances in functional nanomaterials for light–triggered cancer therapy. *Nano Today* **2018**, *19*, 146–187. DOI: 10.1016/j.nantod.2018.02.010.
118. Huang, X.; El-Sayed, I. H.; Qian, W.; El-Sayed, M. A. Cancer cell imaging and photothermal therapy in the near-infrared region by using gold nanorods. *J. Am. Chem. Soc.* **2006**, *128*(6), 2115–2120.
119. Yavuz, M. S.; Cheng, Y.; Chen, J.; Cobley, C. M.; Zhang, Q.; Rycenga, M.; Xie, J.; Kim, C.; Song, K. H.; Schwartz, A. G.; et al. Gold nanocages covered by smart polymers for controlled release with near-infrared light. *Nat. Mater.* **2009**, *8*(12), 935–939. DOI: 10.1038/nmat2564.
120. Zhou, Z.; Wang, Y.; Yan, Y.; Zhang, Q.; Cheng, Y. Dendrimer-Templated Ultrasmall and Multifunctional Photothermal Agents for Efficient Tumor Ablation. *ACS Nano* **2016**, *10*(4), 4863–4872. DOI: 10.1021/acsnano.6b02058.
121. Dumas, A.; Couvreur, P. Palladium: a future key player in the nanomedical field? *Chem. Sci.* **2015**, *6*(4), 2153–2157. DOI: 10.1039/c5sc00070j.
122. Wei, X.; Huang, H.; Guo, J.; Li, N.; Li, Q.; Zhao, T.; Yang, G.; Cai, L.; Yang, H.; Wu, C.; et al. Biomimetic Nano-Immunoactivator via Io nic Metabolic Modulation for Strengthened NIR-II Photothermal Immunotherapy. *Small* **2023**, *19*(49), e2304370. DOI: 10.1002/smll.202304370.
123. Wang, S.; Li, K.; Chen, Y.; Chen, H.; Ma, M.; Feng, J.; Zhao, Q.; Shi, J. Biocompatible PEGylated MoS2 nanosheets: controllable bottom-up synthesis and highly efficient photothermal regression of tumor. *Biomater.* **2015**, *39*, 206–217. DOI: 10.1016/j.biomaterials.2014.11.009.
124. Xuan, J.; Wang, Z.; Chen, Y.; Liang, D.; Cheng, L.; Yang, X.; Liu, Z.; Ma, R.; Sasaki, T.; Geng, F. Organic-Base-Driven Intercalation and Delamination for the Production of Functionalized Titanium Carbide Nanosheets with Superior Photothermal Therapeutic Performance. *Angew. Chem. Int. Ed. Engl.* **2016**, *55*(47), 14569 − 14574. DOI: 10.1002/anie.201606643.
125. Huang, K.; Li, Z.; Lin, J.; Han, G.; Huang, P. Two-dimensional transition metal carbides and nitrides (MXenes) for biomedical applications. *Chem. Soc. Rev.* **2018**, *47*(14), 5109–5124. DOI: 10.1039/c7cs00838d.
126. Lin, H.; Wang, Y.; Gao, S.; Chen, Y.; Shi, J. Theranostic 2D Tantalum Carbide (MXene). *Adv. Mater.* **2018**, *30*(4). DOI: 10.1002/adma.201703284.
127. Chen, R.; Wang, X.; Yao, X.; Zheng, X.; Wang, J.; Jiang, X. Near-IR-triggered photothermal/photodynamic dual-modality therapy system via chitosan hybrid nanospheres. *Biomaterials* **2013**, *34*(33), 8314 − 8322. DOI: 10.1016/j.biomaterials.2013.07.034.
128. Zheng, Y.; Chen, J.; Song, X. R.; Chang, M. Q.; Feng, W.; Huang, H.; Jia, C. X.; Ding, L.; Chen, Y.; Wu, R. Manganese-enriched photonic/catalytic nanomedicine augments synergistic anti-TNBC photothermal/nanocatalytic/immuno-therapy via activating cGAS-STING pathway. *Biomaterials* **2023**, *293*, 121988. DOI: 10.1016/j.biomaterials.2022.121988.